Turun yliopisto
University of Turku

EVOLUTION OF TRANSPORT SPECIFICITY AND POTASSIUM REQUIREMENT IN MEMBRANE PYROPHOSPHATASES

Erika Artukka

TURUN YLIOPISTON JULKAISUJA - ANNALES UNIVERSITATIS TURKUENSIS
Sarja - ser. AI osa - tom. 590 | Astronomica - Chemica - Physica - Mathematica | Turku 2018

Turun yliopisto
University of Turku

EVOLUTION OF TRANSPORT SPECIFICITY AND POTASSIUM REQUIREMENT IN MEMBRANE PYROPHOSPHATASES

Erika Artukka

TURUN YLIOPISTON JULKAISUJA – ANNALES UNIVERSITATIS TURKUENSIS
Sarja - ser. A I osa - tom. 590 | Astronomica - Chemica - Physica - Mathematica | Turku 2018

University of Turku

Faculty of Science and Engineering

Department of Biochemistry

Doctoral Programme in Molecular Life Sciences

Supervised by

Professor Reijo Lahti
Department of Biochemistry
University of Turku
Turku, Finland

Ph.D. Anssi Malinen
Department of Biochemistry,
University of Turku
Turku, Finland

Professor Alexander A. Baykov
A.N. Belozersky Institute of Physico-Chemical Biology
Moscow State University
Moscow, Russia

Reviewed by

Dr. Aurelio Serrano
Instituto de Bioquimica Vegetal y Fotosintesis,
Natl. Res. Council of Spain (CSIC)
University of Seville
Seville, Spain

Professor Masayoshi Maeshima
Laboratory of Cell Dynamics,
Graduate School of Bioagricultural Sciences,
Nagoya University
Nagoya, Japan

Opponent

Professor Markku Kulomaa
Faculty of Medicine and Life Sciences
University of Tampere
Tampere, Finland

The originality of this thesis has been checked in accordance with the University of Turku quality assurance system using the Turnitin OriginalityCheck service.

ISBN 978-951-29-7359-0 (PRINT)
ISBN 978-951-29-7360-6 (PDF)
ISSN 0082-7002 (PRINT)
ISSN 2343-3175 (PDF)
Painosalama Oy – Turku, Finland 2018

> *“The world is full of great and wonderful things for those who are ready for them.”*
> *– Moominpappa*

Contents

List of original publications

I. Luoto HH, **Nordbo E**, Baykov AA, Lahti R & Malinen AM (2013) Membrane Na^+-pyrophosphatases can transport protons at low sodium concentrations. J. Biol. Chem. **288**, 35489–35499.

II. Luoto HH, **Nordbo E**, Malinen AM, Baykov AA & Lahti R (2015) Evolutionarily divergent, Na^+ -regulated H^+ -transporting membrane-bound pyrophosphatases. Biochem. J. **467**, 281–291.

III. **Nordbo E**, Luoto HH, Baykov AA, Lahti R & Malinen AM (2016) Two independent evolutionary routes to Na^+ /H^+ cotransport function in membrane pyrophosphatases. Biochem. J. **473**, 3099–3111.

IV. **Artukka E**, Luoto HH, Baykov AA, Lahti R & Malinen AM (2018) Role of the potassium/lysine cationic center in catalysis and functional asymmetry in membrane-bound pyrophosphatases. Biochem. J. **475**, 1141–1158.

Abstract

My PhD research project focused on membrane-bound inorganic pyrophosphatases (mPPases). mPPases are integral membrane proteins that hydrolyze pyrophosphate (PP_i) and transport H^+ and/or Na^+ ions across membranes thereby forming ion gradients. mPPases are found in bacteria, archaea, protists and plants. mPPases are potential drug targets against parasitic diseases like malaria. Furthermore, mPPases have been shown to improve stress resistance in plants. mPPases can be divided into different subfamilies based on their K^+ requirements and ion pumping specificities. This thesis consists of four articles in which I studied the evolution and functional properties of different mPPase subfamilies.

In the first article we discovered that previously identified Na^+-transporting PPases (Na^+-PPases) are in fact able to transport H^+ ions at low (< 5 mM) Na^+ concentrations. The emergence of the H^+ transport activity was surprisingly not accompanied with a decrease in the Na^+ transport efficiency, suggesting that the two ions do not directly compete for the same ion translocation mechanism. Further enzyme kinetic and mutational analyses led to the identification of two distinct Na^+ binding sites controlling the PP_i hydrolysis and ion transport specificity in Na^+-PPases.

In the second article we focused on a group of mPPases that is phylogenetically distant from other subfamilies. To investigate whether these enzymes are functional mPPases, divergent mPPases from *Chlorobium limicola* and *Cellulomonas fimi* were cloned and characterized. Despite the sequence divergence, these enzymes were identified as functional mPPases that transport H^+ ions and are regulated by Na^+. We concluded that the group of divergent mPPases forms a new subfamily—the Na^+-regulated H^+-PPases.

In the third article we investigated the evolutionary path from Na^+-PPases to mPPases that can transport both Na^+ and H^+ ions (Na^+,H^+-PPases). Ten new enzymes were characterized and classified into subfamilies based on their ion pumping abilities. The first group of Na^+,H^+-PPases was named "Na^+-regulated Na^+,H^+-PPases" as their H^+ transport was inhibited by Na^+. The second group of Na^+,H^+-PPases was named "true Na^+,H^+-PPases" because the Na^+ concentration did not affect their ability to transport H^+. Furthermore, we found that the two differentially regulated groups of double-pumping enzymes have evolved separately.

In the fourth article we showed that the K^+/Lys cationic center, which determines the K^+ dependence of mPPases, is conserved among all mPPase subfamilies. Our mutational analysis revealed that the K^+/Lys center has an important role in PP_i hydrolysis and enhances Na^+ ion binding. Furthermore, our results suggested that substrate inhibition is a result of the allosteric inter-subunit regulation of mPPases and that the K^+/Lys center is part of the regulation mechanism.

Tiivistelmä

Väitöskirjatyössäni tutkin membraanipyrofosfataaseja (mPPaaseja). mPPaasit ovat solukalvon proteiineja, joiden tehtävä solussa on hajottaa pyrofosfaattia (PP_i) ja muodostaa ionigradientteja. mPPaaseja löytyy monista bakteereista, arkeista, kasveista ja alkueliöistä mutta ei ihmisistä eikä muista eläimistä. mPPaasit ovat mahdollisia lääkekohteita esimerkiksi malariaa vastaan, ja niiden on myös havaittu parantavan kasvien stressinsietokykyä. mPPaasit voidaan jakaa alaperheisiin niiden ionipumppausspesifisyyden ja K^+-ioniriippuvuuden perusteella. Tämä väitöskirja koostuu neljästä artikkelista, joissa tutkin eri mPPaasien alaperheiden evoluutiota ja toimintaa.

Ensimmäisessä artikkelissa havaitsin, että Na^+-ioneja pumppaavilla mPPaaseilla eli Na^+-PPaaseilla on kyky pumpata H^+-ioneita matalissa Na^+-ionikonsentraatioissa. H^+-pumppaus ei vähentänyt entsyymin kykyä pumpata Na^+-ioneita, joten nämä kaksi ionia eivät kilpaile samasta sitoutumispaikasta ioninkuljetusmekanismissa. Spesifisten aminohappomuutosten ja kineettisen analyysin avulla päättelimme, että Na^+-PPaaseilla on kaksi erillistä Na^+ ionin sitoutumispaikkaa, jotka ohjaavat PP_i hydrolyysireaktion tehokkuutta ja ioninpumppausspesifisyyttä.

Toisessa artikkelissa tutkin aiemmin tuntematonta mPPaasien alaperhettä, joka on fylogeneettisesti erillään muista alaperheistä. Tämän uuden alaperheen entsyymejä tutkimme *Chlorobium limicola* and *Cellulomonas fimi* bakteereista peräisin olevilla proteiineilla. Tutkimuksessa havaitsimme, että uuden alaperheen entsyymit ovat toimivia mPPaaseja, jotka pumppaavat H^+-ioneita ja että ne ovat Na^+-ioneilla säädeltäviä.

Kolmannessa artikkelissa tutkin, miten mPPaasit, jotka kuljettavat sekä Na^+ että H^+-ioneita (Na^+,H^+-PPaasit), ovat kehittyneet evoluutiossa Na^+-PPaaseista. Fylogeneettisen puun perusteella valittiin 10 entsyymiä, jotka karakterisoitiin. Na^+,H^+-PPaasien havaittiin muodostavan kaksi ryhmää, joista ensimmäinen nimettiin ”Na^+-ioneilla säädeltäviksi Na^+,H^+-PPaaseiksi”, koska niiden H^+-ionipumppauskyky heikkeni Na^+ konsentraation kasvaessa. Toisen ryhmän entsyymit nimettiin ”aidoiksi Na^+,H^+-PPaaseiksi”, koska Na^+-konsentraatio ei vaikuttanut niiden H^+-ionipumppauskykyyn. Lisäksi päättelimme, että nämä kaksi Na^+,H^+-PPaasien alatyyppiä ovat kehittyneet evoluutiossa erikseen.

Neljännessä artikkelissa näytimme, että K^+/Lys keskus, joka määrää mPPaasien K^+-ioniriippuvuuden, on konservoitunut eri mPPaasi-alaperheiden välillä. Aminohappomuutosten avulla selvitimme K^+-aktivaatiomekanismia ja havaitsimme, että K^+/Lys keskuksella on tärkeä rooli PP_i:n hydrolyysissä ja Na^+-ionin sitoutumisessa. K^+-aktivaation todettiin määräytyvän samoin kaikissa mPPaasien eri alaperheissä. Lisäksi tutkimuksessa saatiin tietoa mPPaasien mahdollisesta alayksiköiden välisestä toiminnallisesta mekanismista substraatti-inhibitiossa.

Abbreviations

ACMA	9-Amino-6-chloro-2-methoxyacridine
AMDP	Aminomethylenediphosphonate
ATP	Adenosine triphosphate
CCCP	Carbonyl cyanide 3-chlorophenylhydrazone
$DiBAC_4(3)$	Bis-(1,3-dibutylbarbituric acid)trimethine oxonol
EC	Enzyme commission
EDTA	Ethylenediaminetetraacetic acid
EGTA	Ethylene glycol-bis(2-aminoethylether)-*N,N,N′,N′*-tetraacetic acid
ETH157	N,N′-Dibenzyl-*N,N′*-diphenyl-1,2-phenylenedioxydiacetamide
FRET	Flurescence resonance energy transfer
H^+-PPase	Proton transporting PPase
IDP	Imidodiphosphate
IMV	Inverted membrane vesicles
IPTG	Isopropyl-*β*-D-thiogalactoside
KF	Potassium fluoride
MOPS	3-(*N*-Morpholino)propanesulfonic acid
mPPase	Membrane-bound pyrophosphatase
Na^+-PPase	Na^+-transporting PPase
Na^+,H^+-PPase	Na^+- and H^+-transporting PPase
NCBI	National center for biotechnology information
PDB	Protein data bank
PPase	Pyrophosphatase
PP_i	Pyrophosphate
TMA	Tetramethylammonium
TMH	Transmembrane helix
SD	Standard deviation
sPPase	Soluble PPase
wt	Wild-type

Abbreviations of amino acid residues

A	Ala	Alanine
C	Cys	Cysteine
D	Asp	Aspartate
E	Glu	Glutamate
F	Phe	Phenylalanine
G	Gly	Glycine
H	His	Histidine
I	Ile	Isoleucine
K	Lys	Lysine
L	Leu	Leucine
M	Met	Methionine
N	Asn	Asparagine
P	Pro	Proline
Q	Gln	Glutamine
R	Arg	Arginine
S	Ser	Serine
T	Thr	Threonine
V	Val	Valine
W	Trp	Tryptophan
Y	Tyr	Tyrosine
X		Any amino acid residue

Abbreviations of mPPases

AVP1	*Arabidopsis thaliana* vacuolar H^+-PPase
AVP2	*A. thaliana* K^+ independent H^+-PPase
Bm-PPase	*Brachyspira murdochii* Na^+,H^+-PPase
Bv-PPase	*Bacteroides vulgatus* Na^+,H^+-PPase
Cf-PPase	*Cellulomonas fimi* divergent H^+-PPase
Ch-PPase	*Carboxydothermus hydrogenoformans* H^+-PPase
Cl(2)-PPase	*Chlorobium limicola* divergent H^+-PPase
Clen-PPase	*Clostridium lentocellum* Na^+,H^+-PPase
Clep-PPase	*Clostridium leptum* Na^+,H^+-PPase
Cp-PPase	*Clostridium phytofermentans* Na^+,H^+-PPase
Cyf-PPase	*Cytophaga fermentans* true Na^+,H^+-PPase
Da-PPase	*Desulfuromonas acetoxidans* Na^+-PPase
Dh-PPase	*Desulfitobacterium hafniense* K^+-dependent H^+-PPase
Dl-PPase	*Dehalogenimonas lykanthroporepellens* Na^+-PPase
Fj-PPase	*Flavobacterium johnsoniae* K^+-dependent H^+-PPase
Gs-PPase	*Geobacter sulfurredicencis* K^+-independent H^+-PPase
Ks-PPase	*Candidatus Kuenenia stuttgartiensis* Na^+-PPase
Lb-PPase	*Leptospira biflexa* K^+-dependent H^+-PPase
Ma-PPase	*Mahella australiensis* Na^+,H^+-PPase
Mme-PPase	*Methylomonas methanica* Na^+-PPase
Mm-PPase	*Methanosarcina mazei* Na^+-PPase
Mr-PPase	*Melioribacter roseus* Na^+,H^+-PPase
Oc-PPase	*Oscillibacter valericigenes* Na^+-PPase
Po-PPase	*Prevotella oralis* Na^+,H^+-PPase
Rr-PPase	*Rhodospirillum rubrum* K^+-independent H^+-PPase
Sc-PPase	*Streptomyces coelicolor* K^+-independent H^+-PPase
Ss-PPase	*Shuttleworthia satelles* Na^+-PPase
Tm-PPase	*Thermotoga maritima* Na^+-PPase
Vr-PPase	*Vigna radiata* vacuolar H^+-PPase

1. Introduction

All cells, whether human, bacterial or plant, use ion gradients to power numerous biochemical processes. Ion gradients are electrochemical potential differences of ions across biological membranes. Ion gradients can be utilized by membrane proteins to move the cell, transport nutrients into the cell or to synthetize ATP. Primary pumps are membrane proteins that use chemical or light energy to form ion gradients. This thesis focuses on membrane bound inorganic pyrophosphatases (mPPases). mPPases are primary pumps that use the energy released in pyrophosphate hydrolysis to form H^+ and/or Na^+ ion gradients. mPPases are a functionally versatile group of enzymes that have a unique structure. mPPases are found in bacteria, archaea, protists and plants. mPPases have been used to develop stress resistant plants and they are also possible drug targets against malaria and other parasitic diseases. In my research during this PhD project I studied the functional properties of different mPPases subfamilies. The aim of this research was to understand the evolution, structure and function of this unique enzyme family. In the next section of this thesis I will review the key aspects of mPPase research and then I will present the results obtained in the four publications included in this thesis.

1.1 Discovery of mPPases

mPPases were discovered in the 1960s in the photosynthetic purple bacterium *Rhodospirillum rubrum* in studies of the light-induced formation of pyrophosphate (PP_i) (Baltscheffsky et al., 1966). Further characterization studies revealed that the enzyme is a PP_i-hydrolyzing H^+-transporting mPPase (H^+-PPase) (Moyle et al., 1972; Sarafian et al., 1992). In 1975, mPPases were first found in plants (Karlsson, 1975). Plant H^+-PPases were associated with the vacuolar membrane and found to be different from the *R. rubrum* H^+-PPase in that they needed K^+ ions to function (Rea and Poole, 1986; Walker and Leigh, 1981). Mung bean vacuolar H^+-PPase was the first mPPase obtained in a purified form, allowing its molecular characterization and production of specific antibodies (Maeshima and Yoshida, 1989) and subsequent cloning (Sarafian et al., 1992). In addition to plants, mPPases were discovered in the protozoan *Trypanosoma cruzi* (Scott et al., 1998) and also the archaeon *Pyrobaculum aerophilum* (Drozdowicz et al., 1999).

Genome sequencing and the development of gene cloning techniques enabled the discovery of new mPPase genes that were expressed in *Escherichia coli* and *Saccharomyces cerevisiae* (Belogurov et al., 2002; Kim et al., 1994). As a result, new mPPases were characterized and the functional divergence of mPPases began to unravel. In 2005, the Na^+ activation of some K^+ dependent mPPases was discovered (Belogurov et al., 2005) and two years later the Na^+ transport was first shown (Malinen et al., 2007). The first Na^+-transporting mPPases to be characterized (Na^+-

PPases) were from *Moorella thermoacetica, Thermotoga maritima* and *Methanosarcina mazei* (Malinen et al., 2007). Subsequently, Luoto et al. (2011) established that Na^+-PPases are a widespread subfamily of mPPases. The latest discovered subfamily of mPPases before I started my Ph.D. study were Na^+,H^+-PPases (found in 2013). They are different from other mPPases in that they are able to simultaneously transport both H^+ and Na^+ ions across the membrane (Luoto et al., 2013).

1.2 Function of mPPases

1.2.1 PP_i hydrolysis

Inorganic pyrophosphate (PP_i) is formed in all living cells as a byproduct of many biosynthetic reactions (Heinonen, 2001). Inorganic pyrophosphatases (EC 3.6.1.1) hydrolyze PP_i to yield orthophosphate. Pyrophosphatases can be divided into soluble and membrane bound enzyme families. Soluble PPases (sPPases) form two non-homologous families (I and II). Soluble PPases convert the energy released during PP_i hydrolysis into heat, whereas mPPases use the energy to form ion gradients. However, mPPases are not as effective as sPPases in catalyzing the hydrolysis of PP_i. The typical hydrolysis rate of a mPPase is about 100-1000 times slower than that of sPPases (Kajander et al., 2013). k_{cat} values of around 20 s^{-1} have been reported for mPPases (Maeshima and Yoshida, 1989; Nakanishi et al., 2003; Sato et al., 1994). The reverse reaction, PP_i synthesis, has been measured for the purified H^+-PPase from *R. rubrum* (Rr-PPase) to be 0.6 % (Belogurov et al., 2002) and for the Na^+-PPase from *T. maritima* (Tm-PPase) to be 0.02 % of the PP_i hydrolysis activity (Belogurov et al., 2005). PP_i synthesis is expected to be stimulated in energized membrane. Indeed, Rr-PPase has been shown to function as a PP_i synthase *in vivo* (Baltscheffsky et al., 1966). The pH optimum of mPPases is 6.5-8.0 and it varies slightly between different enzymes (Hirono et al., 2005; Maeshima and Yoshida, 1989; Rodrigues et al., 1999).

mPPases require free Mg^{2+} ions for their enzymatic activity (Maeshima and Yoshida, 1989; Sosa et al., 1992). In the active site, Mg^{2+} ions coordinate PP_i and stabilize the negative charges of the substrate. Two Mg^{2+} ions bind directly to the enzyme and two Mg^{2+} ions bind as a substrate complex. The substrate for mPPase is Mg_2PP_i (Baykov et al., 1993a; Leigh et al., 1992; White et al., 1990). Additionally, PP_i and Mg^{2+} form also other complexes in solution (Gordon-Weeks et al., 1996). Binding of the substrate, Mg_2PP_i, induces conformational changes and protects the enzyme against thermal inactivation (Yang et al., 2004), trypsin digestion and inactivation by mersalyl (Malinen et al., 2008).

Aminomethylenediphosphonate (AMDP) and fluoride have been used to identify mPPase expression in *E. coli* and yeast to distinguish between the PP_i hydrolysis activities of sPPases and mPPases . The PP_i analogue AMDP is known to specifically inhibit mPPases much more strongly than it does soluble PPases (Baykov et al.,

1993b). AMDP is a competitive inhibitor with an apparent inhibition constant of 1.8 µM (Zhen et al., 1994). In contrast, fluoride strongly inhibits sPPases, whereas mPPases are not sensitive to it (Baykov et al., 1993b). This difference is due to structural differences in the active sites of mPPases and sPPases (Lin et al., 2012). Rr-PPase has been shown to be inhibited by 4-bromophenacyl bromide, N,N-dicyclohexylcarbodiimid, diethyl pyrocarbonate and fluorescein 5-isothiocyanate (Schultz and Baltscheffsky, 2003). Also, Ca^{2+} has been shown to inhibit vacuolar H^+-PPase, but not vacuolar ATPase (Maeshima, 1991; Rea et al., 1992). Furthermore, acylspermidine derivatives have been shown to inhibit plant type mPPases (Hirono et al., 2003).

1.2.1.1 K^+ and Na^+ as mPPase activators

K^+ ion dependent H^+-PPases require 30–50 mM K^+ for full activity (Maeshima and Yoshida, 1989). Rb^+ can replace K^+ as the activating ion in both H^+-PPases and Na^+-PPases (Gordon-Weeks et al., 1997; Malinen et al., 2007). Furthermore, NH_4^+, Cs^+, Na^+ and Li^+ ions are able to activate K^+-dependent H^+-PPases (Gordon-Weeks et al., 1997; Obermeyer et al., 1996). K^+ dependence is determined by one conserved amino acid (Belogurov and Lahti, 2002). Mutational studies with K^+ dependent H^+-PPase from *Carboxydothermos hydrogenoformans* showed that replacing the conserved Ala460 residue with Lys converted the enzyme into a K^+-independent form. Interestingly, pyruvate kinases have a similar K^+ dependence mechanism, where the positively charged amino group of lysine can functionally replace the positive charge of K^+, since the Glu→Lys mutation made the K^+ dependent enzyme K^+ independent (Laughlin and Reed, 1997). However, the reverse mutation did not work since the Lys to Ala mutation in a K^+-independent H^+-PPase from *Streptomyces coelicolor* did not convert the K^+ dependence of the enzyme (Hirono et al., 2005).

Na^+-PPases absolutely require Na^+ ions for their hydrolytic activity and they are further activated with millimolar concentrations of K^+ ions (Belogurov et al., 2005; Malinen et al., 2007). Li^+ can substitute Na^+ as the activating ion in Na^+-PPases (Belogurov et al., 2005). In Na^+-PPases, the main effect of the K^+ ion is to increase the affinity for Na^+—in the presence of K^+, less Na^+ is needed for activating the enzyme (Malinen et al., 2007). Kinetic studies with different Na^+-PPases showed that K^+ increases the maximal rate of PP_i hydrolysis 2–10-fold and the Na^+ binding affinity 40–400-fold (Luoto et al., 2011). Na^+-PPases have two binding sites for the Na^+ ion (Malinen et al., 2007). However, the amino acid residues responsible for the Na^+ ion binding have not been unequivocally identified. Asp703 apparently participates in Na^+ ion binding in Tm-PPase. The D703N mutation lowered the maximal activity of the enzyme, and the variant enzyme required more Na^+ for activity compared to the wild-type enzyme (Belogurov et al., 2005). Also, the mutation E242D in Cl-PPase weakened the Na^+ binding (Luoto et al., 2011).

1.2.2 Ion transport

mPPases can transport H^+ ions, Na^+ ions or both (Luoto et al., 2013; Malinen et al., 2007; Moyle et al., 1972). Also, a K^+-transport activity was claimed for mPPases,

but subsequent studies have shown that K^+ ions are not transported across the membrane by vacuolar H^+-PPases or by Na^+-PPases (Malinen et al., 2007; Ros et al., 1995). H^+ transport is a well-studied transport activity of mPPases. The H^+ transport activity has been shown to be electrogenic, and the resulting H^+ gradient can be used for ATP production by the cell. The formation of an electrochemical H^+ potential difference of 270 mV was reported (Ros et al., 1995). Na^+ transport is a quite recently discovered property of Na^+-activated mPPases. Na^+ transport by Na^+-PPases results in the formation of an electrochemical potential gradient, as was shown by experiments with ionophores (Malinen et al., 2007). Na^+,H^+-PPases can transport both Na^+ and H^+ ions. Interestingly, the ability of the Na^+,H^+-PPase to transport both Na^+ and H^+ ions is preserved at different pH and Na^+ concentrations (Luoto et al., 2013). This indicates that there is no competition between the transported ions. It is not clear whether Na^+ and H^+ are transported by different subunits or if both ions are transported simultaneously during the catalytic cycle. Furthermore, the amino acid residues responsible for the ion transport specificity have not been identified. The semi-conserved glutamate is important for the ion transport function but a mutational analysis by Luoto et al. (2011) revealed that it is not solely responsible for the ion transport specificity. The semi-conserved glutamate mutated enzymes Fj-PPase E185S and Lb-PPase E253S were not able to transport H^+ or Na^+ ions (Luoto et al., 2011).

The relative stoichiometry of PP_i hydrolysis and ion transport is not clear. Studies have shown that one or two H^+ ion can be transported for one PP_i molecule hydrolyzed (Nakanishi et al., 2003; Schmidt and Briskin, 1993; Sosa and Celis, 1995). A H^+/PP_i stoichiometry of 1 has been determined for a vacuolar H^+-PPase from *Beta vulgaris* (beetroot) (Schmidt and Briskin, 1993) and a vacuolar H^+-PPase from *Vigna radiata* (mung bean) expressed in recombinant form in yeast (Nakanishi et al., 2003). However, an H^+/PP_i coupling ratio of 2 was measured and calculated for a bacterial K^+-independent H^+-PPase by Sosa and Celis (1995). It is thus possible that H^+-PPases from different subfamilies have different coupling ratios. No coupling ratio for Na^+-PPase has been reported.

1.3 mPPase subfamilies

mPPases can be divided into subfamilies based on their ion requirements and ion pumping specificities (Table 1). The subfamilies have been established by the functional characterization of enzymes as well as sequence comparisons and phylogenetic analyses (Figure 1). The largest subfamily of mPPases is K^+-independent H^+-PPases (Baykov et al., 2013). K^+-dependent H^+-PPases require K^+ ions to be fully functional. They are found in plants and protists but also in bacteria. K^+-dependent enzymes are further divided into H^+ transporters and Na^+ transporters. Na^+-transporting mPPases are fully active in the presence of Na^+ and K^+ ions (Malinen et al., 2007). The Na^+ activation and the ability to transport Na^+ distinguish them from H^+-PPases. Na^+-PPases form the second largest subfamily of mPPases

and are widespread in bacteria and archaea that live in conditions of high temperature or salinity. Na^+,H^+-PPases form their own subfamily and their unique feature is their capability to transport both Na^+ and H^+ ions (Luoto et al., 2013). Na^+,H^+-PPases are found in many anaerobic bacteria that live in the human gut.

Table 1. Examples of characterized mPPases from different subfamilies.

Organism	Subfamily	Organism description	Reference
Streptomyces coelicolor	K^+-independent H^+-PPase	soil-dwelling gram-positive bacterium	Hirono et al., 2005
Rhodospirillum rubrum	K^+-independent H^+-PPase	photosynthetic bacterium	Baltscheffsky et al., 1966
Methanosarcina mazei	Na^+-PPase	methanogenic archaeon	Malinen et al., 2007
Chlorobium limicola	Na^+-PPase	photosynthetic, anaerobic, green sulfur bacterium	Luoto et al., 2011
Thermotoga maritima	Na^+-PPase	thermophilic bacterium	Belogurov et al., 2005
Vigna radiata	plant type H^+-PPase	bean plant	Maeshima and Yoshida, 1989
Arabidopsis thaliana	plant type H^+-PPase	small flowering plant	Sarafian et al., 1992
Flavobacterium johnsoniae	Fj-type K^+-dependent H^+-PPase	anaerobic gram negative soil bacterium	Luoto et al., 2011
Leptospira biflexa	plant type H^+-PPase	non-pathogenic soil and water bacterium	Luoto et al., 2011
Moorella thermoacetica	Na^+-PPase	thermophilic, acetogenic bacterium	Malinen et al., 2007
Pyrobaculum aerophilum	K^+-independent H^+-PPase	hyperthermophilic archaeon	Drozdowicz et al., 1999
Bacteroides vulgatus	Na^+,H^+-PPase	human gut bacterium	Luoto et al., 2013
Trypanosoma cruzi	H^+-PPase	human parasitic protozoan	Hill et al., 2001
Akkermansia muciniphila	Na^+,H^+-PPase	beneficial human gut bacterium	Luoto et al., 2013

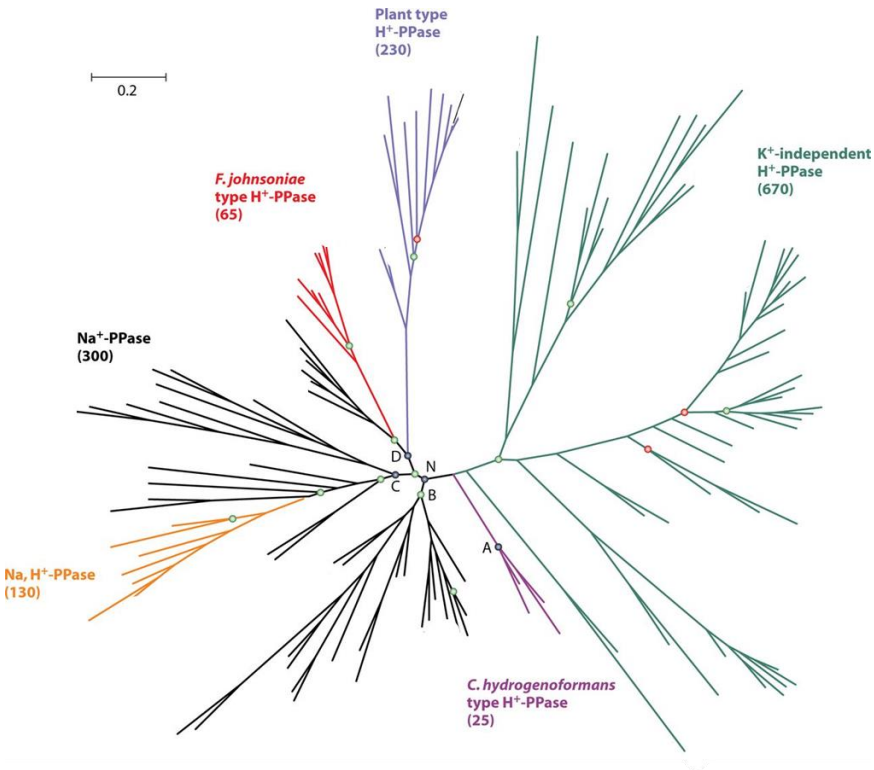

Figure 1. Phylogenetic tree of mPPases. The total number of sequences found in the NCBI protein sequence database in 2013 for each PPase subfamily is given in parentheses. The scale bar represents a 0.2 amino acid substitution per residue. (Reprinted from Baykov et al. Microbiol. Mol. Biol. Rev. 2013;77:267-276 Copyright © 2013, American Society for Microbiology)

The conserved Ala/Lys site can be used to identify K^+-dependent and independent subfamilies. In a H^+-PPase from *C. hydrogenoformans* the signature site for K^+ dependence is Ala460 (Belogurov and Lahti, 2002). K^+ independent H^+-PPases have Lys in the Ala position. K^+ dependent H^+-PPases form three subfamilies in the phylogenetic tree. *C. hydrogenoformans*-type, *Flavobacterium johnsoniae*-type and plant-type K^+-dependent H^+-PPases form three different subfamilies, the first two having been named after their representative characterized members (Luoto et al., 2011). These subfamilies are functionally similar but can be distinguished from each other based on a semi-conserved glutamate residue in sequence alignments. The glutamate is found near the ion gate at a slightly different position in the different subfamilies, is important for ion transport specificity and conserved within subfamilies. In the plant type H^+-PPases, the glutamate is found in transmembrane helix 6 (TMH 6) (Glu301, *V. radiate* numbering). In Fj-type H^+-PPases, the conserved glutamate is not found in TMH 6 but in TMH 5 (Luoto et al., 2011), and in Na^+-PPases, the glutamate is located near the end of TMH 6 (Glu246, *T. maritima* numbering). The most recently discovered subfamily of Na^+,H^+-PPases possesses four signature residues: Thr90, Phe94, Asp146, and Met176 (*B. vulgatus*-numbering)

(Luoto et al., 2013). These residues are apparently conserved and found in all enzymes of the Na^+,H^+-PPase subfamily.

1.4 Evolution of mPPases

mPPases have possibly evolved through a gene duplication event, as can be deduced from the homology between TMHs 5–6 and 15–16 and the loops between them (Hedlund et al., 2006; Kellosalo et al., 2012). Furthermore, the mPPase sequence is abundant in the evolutionarily old amino acids Gly, Ala, Asp and Val (Hedlund et al., 2006; Serrano et al., 2004). All in all, mPPases are thought to be evolutionarily old enzymes. They are found in organisms from all three domains of life and therefore are likely to have evolved before the divergence to bacteria, archaea and eukaryotes (Drozdowicz and Rea, 2001). It has been speculated that mPPases were present in the last universal common ancestor (LUCA) and also in a pre-LUCA extremophile (Baltscheffsky and Persson, 2014; Seufferheld et al., 2011).

It has been proposed that PP_i could have preceded ATP in the initial evolution of life on Earth (Holm and Baltscheffsky, 2011). Furthermore, it has been speculated that early life would have evolved using Na^+ rather than H^+ bioenergetics (Mulkidjanian et al., 2008). mPPases fit into this model as H^+ PPases that have likely evolved from Na^+-PPases (Luoto et al., 2011). Presumably, the first mPPase was a K^+-dependent Na^+ transporter. The ability to transport H^+ ions evolved possibly from Na^+,H^+ PPases with some modifications in the ion channel that enabled also H^+ ions to be pumped (Luoto et al., 2013). Exclusive H^+ pumping has evolved independently at least three times forming the different K^+ dependent H^+-PPase subfamilies that have the semi-conserved glutamate in different positions (Luoto et al., 2011).

1.5 Physiological significance

mPPases work in parallel with ATPases to maintain ion gradients across membranes. On the other hand, mPPases work together with sPPases to hydrolyze PP_i in cells. PP_i hydrolysis is essential for all cells because the accumulation of PP_i would inhibit biosynthetic reactions (Heinonen, 2001). H^+-PPase can functionally replace sPPase as PP_i hydrolyzing enzyme in yeast (Perez-Castineira et al., 2002). The two PP_i hydrolyzing enzymes, mPPases and sPPases, are differentially regulated in the cell (López-Marqués et al., 2004). mPPases have different physiological locations in plants, protists and prokaryotes. In prokaryotes, mPPases are found in the plasma membrane, where they transport ions to the periplasmic space. In plants and protists, mPPases are found in the vacuolar or acidocalcisome membrane in addition to the plasma membrane (figure 2).

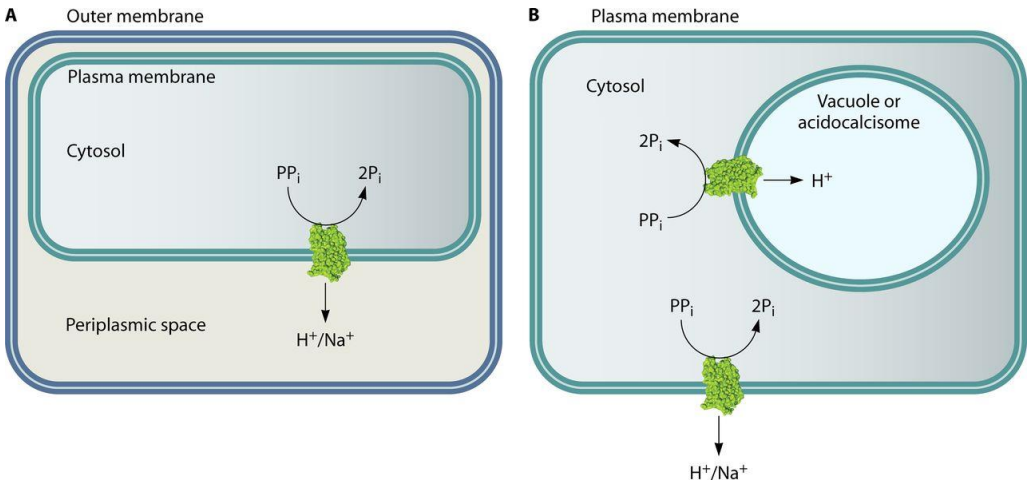

Figure 2. Location of mPPases in prokaryotic cells (A) and eukaryotic cells (B). Reprinted from Baykov et al. Microbiol. Mol. Biol. Rev. 2013;77:267-276 Copyright © 2013, American Society for Microbiology

1.5.1 mPPases in prokaryotes

mPPases of all different subfamilies are found in prokaryotes (Luoto et al., 2011), but they are distributed between them sporadically. Even within the same genus, some species have an mPPase gene, while others do not. This is probably due to a lineage specific loss of mPPase genes or to a lateral gene transfer event (Baykov et al., 2013; Nelson et al., 1999). In many cases, mPPases are found in bacteria and archaea that live in extreme conditions such as high temperatures or high salinity (Serrano et al., 2004). mPPases hydrolyze PP_i to create an H^+ and/or Na^+ ion gradient across the cell membranes in prokaryotes and can replace ATPases in conditions of low energy. They have an important role during fermentative growth (Bielen et al., 2010; Schöcke and Schink, 1998). For example, transforming the energy released during PP_i hydrolysis into an Na^+ ion gradient has an important role in the caffeate respiration in *Acetobacterium woodii* (Biegel and Muller, 2011).

According to one view, organisms that live at high temperatures would prefer Na^+-based bioenergetics over H^+, because the cell membranes become leaky for protons at high temperatures. However, there is no direct correlation between the temperature of the environment and the mPPase pumping specificity. For example, a mPPase from *Pyrobaculum aerophilum* is believed to transport H^+ despite the high temperature that the host organism has adapted to (Drozdowicz et al., 1999). Interestingly, an analysis by Luoto *et al.* (2011) suggests that Na^+-transporting mPPases are more frequently found in organisms living in anaerobic and high-salt conditions. Na^+-PPases can help to pump excess Na^+ ions out of the cell.

H^+-PPase from *R. rubrum* can function in the direction of H^+-transport or PP_i synthesis depending on the growth conditions (Baltscheffsky et al., 1966). In aerobic conditions when light is available, H^+-PPase acts as a PP_i synthase, whereas in anaerobic and low-light conditions H^+-PPase maintains the H^+ gradient. *R. rubrum*

cells producing a mutant H^+-PPase grow slowly in low-light and anaerobic conditions (Garcia-Contreras et al., 2004). Furthermore, salt stress increases the expression of mPPase in *R. rubrum* (López-Marqués et al., 2004). *E. coli* and *S. cerevisiae* do not have genes for mPPases, but their genetically engineered versions expressing plant H^+-PPases demonstrated enhanced tolerance against salt stress (Yoon et al., 2013). Furthermore, the expression of a Na^+,H^+-PPase from *Clostridium methylpentosum* improved salt tolerance in *E. coli*, *S. cerevisiae* and the tobacco plant (Yang et al., 2016). This indicates that mPPases can help the host to cope under stress conditions, but that mPPases are not essential for prokaryotes.

1.5.2 mPPases in plants

Both K^+-dependent and K^+-independent H^+-PPases are found in plants. These two types of enzymes have been characterized in *Arabidopsis thaliana* and they are named AVP1 and AVP2. AVP1 is found in the vacuolar membrane, whereas AVP2 is found in the membrane of the Golgi apparatus (Segami et al., 2010). AVP1 is a K^+ dependent H^+-PPase (Sarafian et al., 1992), and AVP2 is not its isoform but a separate type of an K^+-independent H^+-PPase (Drozdowicz et al., 2000). The expression level of AVP2 is low compared to AVP1 (Segami et al., 2010). H^+-PPase studies in plants have mainly focused on the vacuolar type enzymes. Vacuolar H^+-PPases acidify the plant vacuole and are able to functionally complement vacuolar ATPases (Kriegel et al., 2015; Pérez-Castiñeira et al., 2011; Rea and Sanders, 1987). Vacuolar H^+-PPases have important role in maintaining low levels of PP_i to drive biosynthesis reactions in the cytosol (Segami et al., 2018).

Overexpression of AVP1 increases the size of the plant, whereas plants, where AVP1 expression has been knock-down, do not grow properly (Gaxiola et al., 2001). Vacuolar H^+-PPase has an important role during the development of the plant, and PP_i hydrolysis by an H^+ PPase is needed in postgerminative growth (Ferjani et al., 2011). Auxin-mediated growth enhancement has been suggested as an explanation for the larger size of the plants overexpressing a vacuolar H^+-PPase (Li et al., 2005). In other studies, the PP_i hydrolysis function has been suggested as the main regulatory function of the vacuolar H^+-PPase (Ferjani et al., 2011). Accordingly, overexpression of a mutant vacuolar H^+-PPase, that exhibits defective pumping, increased the size of the plants (Asaoka et al., 2016). Recent studies have also indicated that H^+-PPase overexpression has an effect on sucrose transport (Khadilkar et al., 2016; Pizzio et al., 2015).

Overexpression of a vacuolar H^+-PPase has been used to engineer plants that have increased stress tolerance against cold, salt, nutrient deprivation and drought (Gamboa et al., 2013; Lv et al., 2009; Park et al., 2005). Interestingly, H^+-PPases are naturally found in a halotolerant alga (Meng et al., 2011) and halophytic grass (Rauf et al., 2017). The overexpression of a transgenic H^+-PPase has also been shown to increase the bio-mass of plants in a saline field (Schilling et al., 2014). Under Na^+ stress, a plant cell can maintain its cytosolic functions by accumulating excess Na^+ into the vacuole (Fukuda et al., 2004; Silva and Gerós, 2009). H^+-PPases can help

plants tolerate salt stress by working together with a vacuolar Na^+/H^+ antiporter. Accordingly, the transgenic expression of a vacuolar H^+-PPase together with a Na/H^+ antiporter improved salt and drought resistance in *Medicago sativa L*. (alfalfa) and in *A. thaliana* (Brini et al., 2007; Liu et al., 2013).

All in all, numerous studies have shown the effect of mPPase modifications on the stress resistance and growth of the plants. However, the molecular level explanation for this is not yet clear. Vacuolar H^+-PPases likely have many roles, and the mechanism of growth enhancement is probably complex because of the differences in the regulation of vacuolar PPase genes in different cell types and during different developmental phases in plants (Gaxiola et al., 2016; Schilling et al., 2017).

1.5.3 mPPases in protists

In protists, H^+-PPases are found in the plasma membrane, Golgi apparatus and acidocalcisome membranes (Martinez et al., 2002; Rodrigues et al., 1999; Scott et al., 1998). Acidocalcisomes are special cell organelles that contain an acidic solution rich in polyphosphate and Ca^{2+} ions and have an important role in the control of the pH and osmotic balance of the cell (Docampo and Moreno, 2011). Like plants, protists may encode two different kinds of mPPases in their genome. The type 1 enzymes are located to the acidocalcisome membrane and are similar to the vacuolar H^+-PPases found in plants. For example, *Plasmodium falciparum* has two mPPase genes (PfVP1 and PfVP2), of which PfVP1 is expressed more on both the mRNA and protein levels (McIntosh et al., 2001). mPPases have a key role in the survival of protists especially during osmotic stress and under changing salt levels. mPPase is essential for adaptation to salt stress during the endoparasitic phase of *Philasterides dicentrarchi* (Mallo et al., 2016). Furthermore, when H^+-PPase was silenced with RNA interference in *Trypanosoma brucei*, the acidocalcisome acidification was found defective and the silenced cells grew slower than controls (Lemercier et al., 2002).

1.5.4 mPPases as drug targets

mPPases are found in many human disease-causing protozoan parasites. These diseases include malaria, toxoplasmosis, trypanosomiasis and leishmaniasis. mPPases are crucial for the survival of several disease-causing parasites and for their ability to infect (Lemercier et al., 2002; Liu et al., 2014). Importantly, mPPases are not found in humans and consequently they are promising drug targets against parasitic diseases (Martin et al., 2001; Rodrigues et al., 1999; Shah et al., 2016). Different bisphosphonates have been shown to inhibit the growth of *Plasmodium falciparum, Toxoplasma gondii, Trypanosoma brucei, Trypanosoma cruzi* and *Leishmania donovani* (Martin et al., 2001). In addition, an H^+-PPase inhibiting drug was successfully used to treat a protozoan borne disease in cultured turbot fish (Mallo et al., 2016).

mPPases are also present in pathogenic bacteria like *Bacteroides fragilis* and *Clostridium tetani*. Presumably, mPPases are not essential for the bacteria, so drugs that inhibit the function of mPPases would have only little effect on the survival of

the bacteria. Instead, a prospective drug molecule that binds to mPPase and opens its ion channel, thereby disturbing the ion gradient across the membrane, would have a dramatic effect on the cellular functions of the bacteria (Shah et al., 2016).

1.6. 3-D Structure of mPPases

mPPases exist as dimers (Maeshima, 1990; Mimura et al., 2005; Sato et al., 1991; Tzeng et al., 1996; Wu et al., 1991) (Figure 3A). The dimerization is important for their function, and coupling to a defective subunit lowers the activity of the enzyme (Yang et al., 2000, 2004). A mPPase monomer is constructed of 650 to 900 amino acid residues forming 16 transmembrane helices that are arranged into two concentric rings. The inner ring is formed by TMHs 5, 6, 11, 12, 15 and 16 (Kellosalo et al., 2012; Lin et al., 2012) (Figure 3B). A mPPase is tightly bound to the membrane due to its hydrophobicity (Figure 3C). Accordingly, purified mPPases require phospholipids (Maeshima and Yoshida, 1989) or a suitable detergent molecule (Kellosalo et al., 2011) to remain functional.

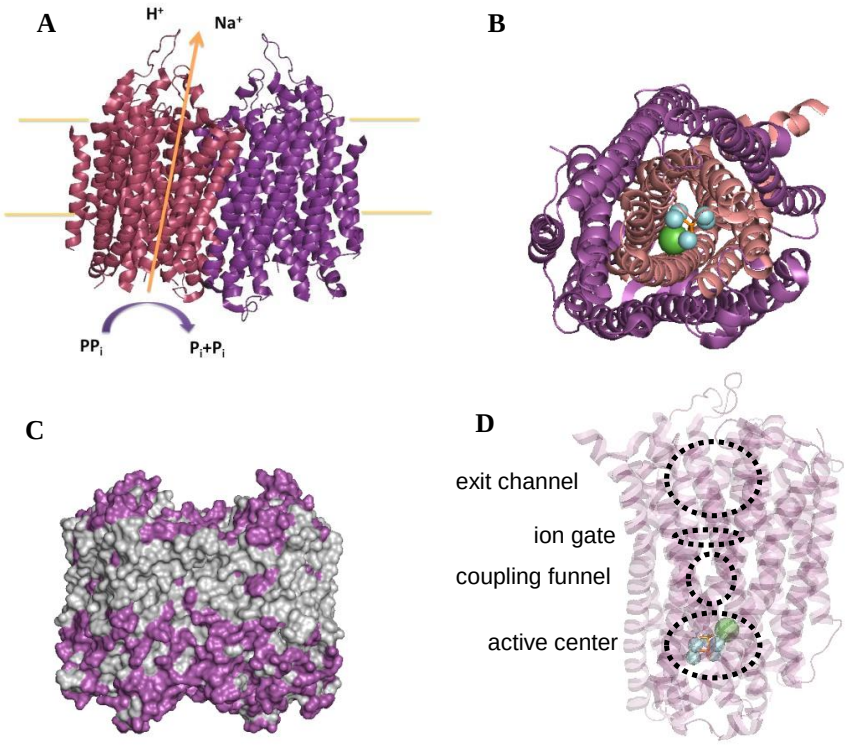

Figure 3. A) mPPase dimer. The yellow line indicates the membrane boundaries. B) Cytosolic view of a mPPase monomer. The inner TMHs are colored in light pink. Mg^{2+}, K^{+} and IDP are in cyan, green and orange, respectively. C) The hydrophobic residues of the mPPase dimer are colored in gray D) functional sites of a mPPase monomer. All figures were created from PDB ID: 4A01 using PyMOL (DeLano, 2002).

mPPases have a unique structure that does not resemble that of any other protein family. The 3-D structure of a mPPase has been solved by x-ray crystallography for two different kinds of enzymes – a plant type H^+-PPase from *V. radiata* (mung bean) (Lin et al., 2012) and a Na^+-PPase from the thermophilic bacterium *T. maritima* (Kellosalo et al., 2012). There are currently six different structures for these mPPases in the protein data bank (Table 2). These structures represent different conformations with different ligands. The structures show the binding of the substrate analogue IDP, the product P_i and activating ions Mg^{2+}, K^+ and Na^+. Four functional sites can be found in the core of the mPPase TMH bundle: the active center where the substrate binds, the coupling funnel, the ion gate and the exit channel (Figure 3 D).

Table 2. All currently available mPPase structures found in PDB.

PDB code	organism	resolution (Å)	ligands	conformation	reference
5GPJ	*Vigna radiata*	3.5	Mg^{2+}, PO_4	product bound	(Li et al., 2016)
5LZQ	*Thermotoga maritima*	3.49	IDP, Mg^{2+}, Na^+	substrate analogue bound	(Li et al., 2016)
5LZR	*Thermotoga maritima*	4.0	WO_4, Mg^{2+}	product analogue bound	(Li et al., 2016)
4AV3	*Thermotoga maritima*	2.6	Ca^{2+}, Mg^{2+}	resting state	(Kellosalo et al., 2012)
4AV6	*Thermotoga maritima*	4.0	PO_4, K^+, Mg^{2+}	product bound	(Kellosalo et al., 2012)
4A01	*Vigna radiata*	2.35	Decylmaltoside, IDP, Mg^{2+}, K^+	substrate analogue bound	(Lin et al., 2012)

In the active center of Vr-PPase (Figure 4 A), the substrate analogue imidodiphosphate (IDP) is coordinated by five Mg^{2+} ions and three conserved lysine residues: Lys250, Lys694 and Lys730 (Lin et al., 2012). A water molecule is coordinated by conserved aspartates (Asp287 and Asp731) near the substrate binding site. Hydrolysis is mediated by a nucleophilic water attack (Cooperman 1992, Kajander 2013). Also a K^+ ion is found in the active site. K^+ coordinates and increases the electrophilicity of a phosphate residue for the nucleophile attack in the hydrolytic center (Kellosalo et al., 2012). When the substrate is bound, the active center is closed by the loop between TMHs 5 and 6 (Figure 4 C, D).

The coupling funnel is lined with conserved negatively charged asparagine residues. The 20-Å long funnel connects the hydrolytic center to the ion gate (Kellosalo et al., 2012). In Tm-PPase, an Asp-Lys-Glu triad (Figure 4B) and in Vr-PPase an Asp-Lys pair form the gate to the ion transporting channel (Kellosalo et al., 2012; Lin et al., 2012). The gate structure determines the specificity of the ion transport. Interestingly, a similar Asp-Arg/Lys pair is important for proton selection in a voltage-gated proton channel (Dudev et al., 2015). The exit channel of a mPPase is hydrophobic and contains no conserved amino acid residues. The exit channel and

ion gate are closed in all available structures. Superimposed structures of Tm-PPases with the substrate bound and in the resting state are shown in Figure 4 C. Binding of the substrate changes the conformation, as is indicated by the movements of the TMHs, especially of TMHs 11 and 12, and the cytoplasmic loop 5-6 that closes the active site. The gate residue Lys707 also moves up as a result of substrate binding (Figure 4 D).

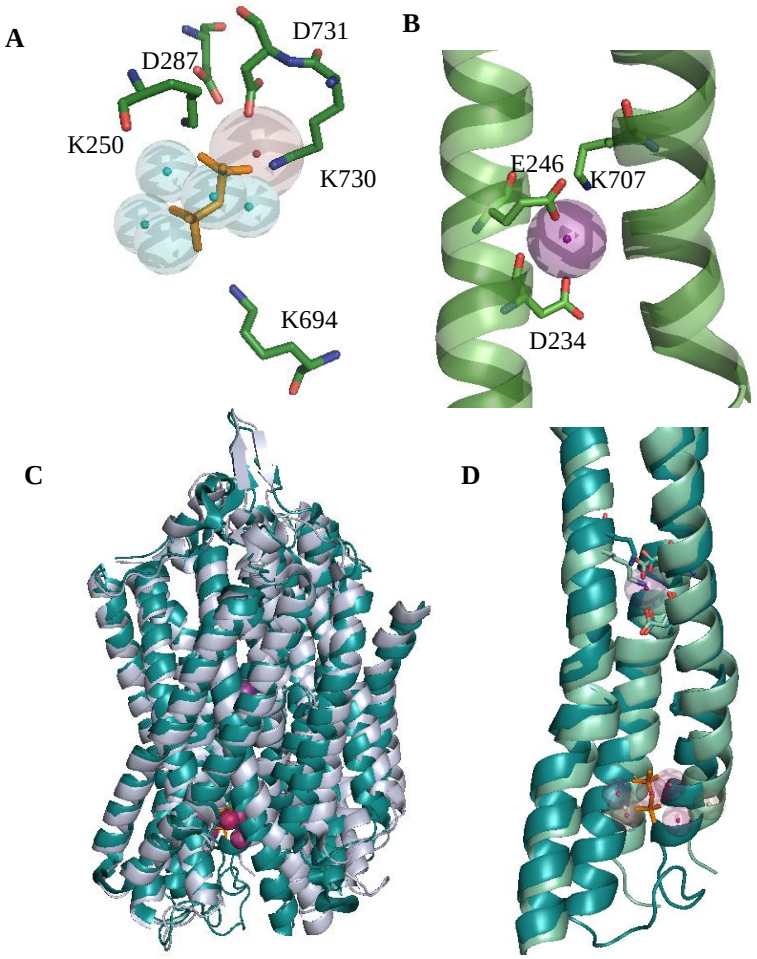

Figure 4. Vr-PPase (4A01) active center. IDP in orange, Mg^{2+} in cyan, and K^{+} in brown. B) The Tm-PPase gate residues and the Na^{+} ion in purple. C) The superimposed structures of Tm-PPase 5LZQ in darker and 4AV3 in pale blue. Mg^{2+} ions in pink. D) The superimposed TMHs 5, 6 and 12 and gate residues. All figures were created using PyMOL (DeLano, 2002).

1.6.1 Functionally important amino acid residues

Amino acid residues that are important for the function of mPPases have been identified by mutational analyses. Many of these residues are highly conserved. The active site and coupling funnel contain the majority of the functionally important

conserved residues. Asaoka *et al.* (2014) performed a wide mutational analysis of Vr-PPase and demonstrated the essential role of several residues near the substrate-binding site (Thr249, Asp269, Asp507 and Asn534) and the H^+ translocation pathway (Ile545, Leu555, Asn738, Val746 and Leu749). Furthermore, they identified two mutations that uncoupled PP_i hydrolysis and H^+-transport (Ile545A and Leu749A) (Asaoka et al., 2014).

The conserved DX_7KXE motif and the loop between TMHs 5 and 6 are important for the function of mPPases. Many of the amino acid residues found in the loop have been shown to be important for the hydrolysis function. Residues Asp253, Lys261, and Glu263 are needed for the function and Lys261 and Glu263 for binding the substrate (Nakanishi et al., 2001) in Vr-PPase. Lys250 is important for PP_i binding and is the main target for trypsin digestion in Vr-PPase (Lee et al., 2011).

An extensive mutational analysis of Sc-PPase identified Thr409, Val411, and Gly414 as essential for optimal function. Phe388, Thr389, and Val396 are needed for efficient H^+ transport. Ala436 and Pro560 have a role in the coupling of PP_i hydrolysis and H^+ transport. Pro189, Asp281, and Val351 are needed for the function and Gly198, Glu262, Gly294, Ser325, Gly374, and Leu377 proved to be important for the PP_i hydrolysis and proton-pumping activities (Hirono et al., 2007b, 2007a).

In all of the cases described above, the mutation reduced the activity of the enzyme drastically, but some mutations proved to enhance the function of the mPPase. Thus, the F388Y and A514S mutations improved the activity and the coupling ratio of the Sc-PPase (Hirono and Maeshima, 2009).

1.7 Mechanism of ion transport

While the mechanism of hydrolysis by soluble PPases is understood well (Baykov et al., 2017; Oksanen et al., 2007), the ion transport mechanism of mPPases remains to be solved. Despite the evident functional similarity between well-characterized F_1F_o-ATPases and mPPases (both couple the hydrolysis of a phosphoanhydride to ion transport), their mechanisms are principally different because of the unique structure of the mPPases.

Studies using an smFRET technique have shown that a mPPase has at least three conformations during its catalytic cycle (Huang et al., 2013). Based on the 3D-structures, closure of the active site as a result of PP_i binding is mainly due to the movement of TMHs 5, 6 and 12 (Kellosalo et al., 2012; Tsai et al., 2014). The loops between TMHs 5–6 and 13–14 bend over the active site to close it. Presumably, the closure of the active center is a critical step in the catalytic cycle and links hydrolysis to conformational changes (Shah et al., 2017). The questions that remain are: how is the PP_i hydrolysis coupled to ion transport and what is the order of the hydrolysis and transport events? Three different mechanisms have been proposed.

Li *et al*. (2016) have proposed a "Grotthuss type" mechanism of proton wiring for the transport, resembling that found in bacteriorhodopsin (Luecke, 1998). In this mechanism, PP_i hydrolysis induces H^+ pumping through a proton wire inside the ion channel. The proton does not move physically but instead the pumping is the result of a series of the breaking and forming of O-H bonds. However, it is not clear if the transported H^+ ion is the same as the proton released from the water nucleophile during PP_i hydrolysis or a separately bound ion. Also this model does not explain Na^+ transport, and the conserved structure between prokaryotic and plant type mPPases indicates a conserved mechanism for the H^+ and Na^+ transport (Li et al., 2016).

Baykov *et al.* (2013) have proposed a unifying mechanism for both H^+ and Na^+ transport. They suggested that a proton generated during PP_i hydrolysis could be directly transported (a direct Mitchelian coupling, as opposed to Boyer's indirect coupling in F_1F_o-ATPases). In Na^+-transporting mPPases, the proton pushes out the Na^+ ion to be transported and dissipates in the medium in the Na^+-PPases, or is transported along with the Na^+ ion in the Na^+,H^+-PPases. This mechanism assumes that the PP_i hydrolysis step precedes the ion transport step. An alternative interpretation proposes that in Na^+,H^+-PPases H^+ pumping by one subunit would allosterically induce the pumping of Na^+ by the other subunit (Li et al., 2016; Luoto et al., 2013).

Kellosalo *et al*. (2012) proposed a binding change mechanism (Figure 5). In this mechanism, substrate binding induces the opening of the ion transport channel, allowing the transport of the H^+ or Na^+ ion already present there. This mechanism differs from the above-described mechanisms in that it assumes that the transport event is induced by substrate binding and precedes the hydrolysis step. This mechanism was further elaborated in more recent publications (Hsu *et al.*, 2015; Li *et al.* 2016; Shah *et al.*, 2017). While the other mechanisms are purely speculative, the mechanism of Kellosalo *et al*. is supported by the electrometric observation that binding of the substrate analogue IDP to Vr-PPase does result in a small potential difference across the membrane. This effect, however, may have a different origin, given the involvement of interactions between the enzyme and multiple charged metal ions (Mg^{2+} and K^+) on the one hand, and between the charged IDP molecule and one or two Mg^{2+} ions on the other. The observed potential difference may result from a change in the equilibria of these interactions upon IDP binding. The implications of this mechanism for the reverse reaction of PP_i synthesis have been described (Regmi et al., 2016).

The fine details of how PP_i hydrolysis is coupled to the ion transport step and what determines the specificity of Na^+/H^+ ion pumping thus remain to be solved. It is, however, clear that any hypothetical mechanism of transport should explain both H^+ and Na^+ transport.

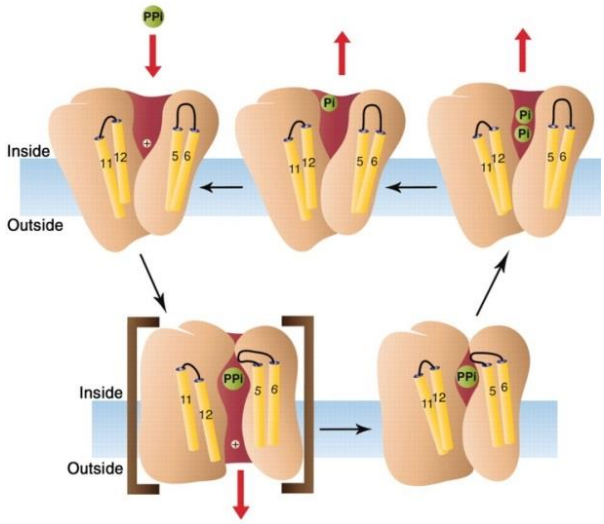

Figure 5. Binding change type mechanism of mPPase ion transport. Reprinted with permission from Kellosalo, J., Kajander, T., Kogan, K., Pokharel, K. and Goldman, A. (2012) 'The structure and catalytic cycle of a sodium-pumping pyrophosphatase', *Science*. 2012/07/28, 337(6093), pp. 473–476. Reprinted with permission from AAAS, Copyright © 2012, American Association for the Advancement of Science

2. Aims of the study

The first aim of my Ph.D. thesis research project was to characterize the ion transport mechanism and specificity of Na^+-PPases using functional assays in combination with mutational analyses.

The second aim was to characterize the previously unknown evolutionary divergent group of enzymes that are only 30 % identical to other mPPase sequences. The goal was to clarify whether these enzymes are functional mPPases and to investigate if they have any unusual characteristics.

The third aim of the project was to investigate the evolutionary path from Na^+-PPases to Na^+,H^+-PPases by experimentally determining the ion transport specificities of several representative enzymes in the corresponding area in the phylogenetic tree for mPPases . When our preliminary data had revealed the existence of two types of Na^+,H^+-PPases, the aim was expanded to include a detailed functional characterization of both Na^+,H^+-PPase subfamilies.

The fourth aim was to elucidate the mechanistic basis of the K^+ dependence in all mPPase subfamilies and how it has changed during evolution.

3. Materials and Methods

3.1 Bioinformatics

mPPase protein sequences were retrieved from the NCBI database using a BLAST search (Altschul et al., 1990). The Rr-PPase or Bv-PPase sequence was used as the query. Sequences were aligned using the MUSCLE multiple alignment program (Edgar, 2004). Sequences that were over 90 % similar were usually removed. Sequence alignments were manually trimmed so that only the areas with reasonably conserved amino acid residues remained. Next, the alignment sets were used as input for calculating phylogenetic trees with MrBayes 3.2.1 (Ronquist and Huelsenbeck, 2003) or RaxML (Stamatakis et al., 2008).

3.2 Expression of mPPases and the preparation of IMVs

Membrane PPase encoding genes were cloned by PCR from genomic DNAs obtained from the Leibniz Institute DSMZ - German Collection of Microorganisms and Cell Cultures. In cases where the genomic DNA was not available, synthetic genes were ordered from Eurofins. Specific primers were ordered from TAG Copenhagen. The Nde I and Xho I restriction sites were utilized when possible to clone the genes into the pET36b vector. Cloning was verified by sequencing the part of the plasmid containing the mPPase gene. The *E. coli* XL1-Blue strain was used for plasmid copying. Mutations were introduced into the genes with specific primers.

The mPPase proteins were expressed in the *E. coli* C41(DE3) strain (Miroux and Walker, 1996) carrying an additional pAYCA-RIL plasmid encoding transfer RNA's that are rare in *E. coli* (Belogurov et al., 2005). The expression was induced with 0.2 mM IPTG and continued for 4–5 h. Cells were harvested by centrifugation at 4500 x g for 15 min and washed with 10 % glycerol three times to remove the growth medium. Inverted membrane vesicles (IMVs) were prepared with some modifications according to Belogurov *et al*. (2005). Cells were suspended in 10 mM MOPS-TMAOH buffer, pH 7.2, containing 0.15 M sucrose, 1 mM $MgCl_2$, 5 mM DTT, and 50 µM EGTA. DNAse I was added and the cells were broken with a French press using a pressure of 1000 psi. Cell debris was then removed by centrifugation at 40 000 x g for 30 min. The supernatant was transferred to an ultracentrifuge tube, and a 2 ml gradient of 900 mM sucrose was added to the bottom of the tube. The tubes were then ultracentrifuged for 2 h at 42 000 rpm using a 50.2.Ti rotor. The centrifugation was repeated three times and a new gradient was added between the runs. Notably, approximately one half of the vesicles isolated by centrifugation were inverted vesicles. Finally, the gradient pillow containing the IMVs was collected and frozen in aliquots in Eppendorf tubes in liquid nitrogen. The IMVs were quantified by determining the total protein concentration using the Bradford method.

The expression of mPPase proteins was verified with western blotting (Malinen et al., 2007). A vesicle sample containing 10 µg/µl protein was denaturated in SDS buffer at 50 °C for 15 min and loaded to a SDS-PAGE gel (4–20 %). After electrophoresis, the proteins were transferred to a nitrocellulose membrane (0.4 µm)

using a semi-dry blotter. The membrane was placed in blocking solution containing 5 % milk powder in 100 mM Tris-HCl, pH 7.6, 0.1 % Tween-20 buffer. After incubating for 16 h at 4 °C, the membrane was rinsed with water and an antibody raised against the conserved H^+-PPase peptide sequence IYTKAADVGADLVGKVE was added and incubated for 1 h at 22 °C. The membrane was then rinsed with a buffer containing 100 mM NaCl, 100 mM Tris-HCl, pH 7.6 and 0.05 % Tween-20. Finally, the secondary anti-rabbit antibody was added and incubated for 1 h. The membrane was scanned with an Odyssey infra-red imager.

3.3 Hydrolysis activity assay

E. coli does not have a mPPase, and soluble PPase is washed away during vesicle preparation, so native *E. coli* vesicles could be directly used in PP_i activity measurements. Mg^{2+}, K^+ and Na^+ form different kinds of complexes with PP_i. Association constants for the PP_i complexes were taken into account when calculating the pipetted amounts of the reagents (Baykov et al., 1993a). Care was taken not to exceed the solubility limit of the Mg_2PP_i complex when planning the experiments.

Hydrolysis activity was measured with a semi-automatic P_i analyzer (Baykov and Avaeva, 1981) at 25 °C. The analyzer continuously withdraws reaction medium, mixes it with sulfuric acid/molybdate and methyl green solutions and measures the resulting absorbance at 660 nm in a flow photometer. Changes in the absorbance are proportional to the P_i concentration. A typical reaction mixture contained 100 mM MOPS-TMAOH, pH 7.2, 40 µM EGTA, 5 mM Mg^{2+}, 0-200 mM K^+, 0-200 mM Na^+, 0,5-1000 µM Mg_2PP_i. The reaction was started by adding vesicles and the reaction rate was determined from the linear change in absorbance per second. The reactions were typically monitored for 4 min. Reaction rates were calculated from the initial slopes of recorder tracings.

Trypsin inactivation of mPPase was measured with a trypsin to IMVs ratio of 1:10. IMVs were incubated with trypsin at 37 °C in the presence of 50 mM K^+ or 100 µM imidodiphosphate. The hydrolysis activity of the IMVs was monitored in aliquots at different time points.

3.4 H^+ transport assay

H^+ transport was measured with a fluorimeter at 22 °C using the fluorescent dye ACMA. The reaction mixture typically contained 20 mM MOPS-TMAOH, pH 7.2, 8 µM EGTA, 5 mM Mg^{2+}, 300 µM Mg_2PP_i, 0–50 mM K^+, 0–100 mM Na^+, 20 µM ACMA and 0.15–0.3 mg/ml of vesicles. The excitation wavelength was 428 nm and emission 475 nm. The reaction was incubated for 4 min in the dark and then 2 min in light before PP_i was added. The decline in the fluorescence indicated the accumulation of the H^+ ion in the vesicles. The signal was restored by adding 10 mM NH_4Cl which cleared the H^+ gradient through the native *E. coli* NH_4^+/H^+ transporter.

Alternatively, $DiBAC_4(3)$ was used as the fluorescent probe instead of ACMA to measure changes in membrane potential.

3.5 Na^+ transport assay

Na^+ transport was measured with ^{22}Na at 22 °C. Typically, 1 mg/ml IMVs in 20 MOPS-TMAOH, pH 7.2, 8 µM EGTA, 50 mM K^+, 1 mM Na^+, 5 mM Mg^{2+} was incubated with $^{22}NaCl$. The transport reaction was initiated by adding 10 µl PP_i or for the control reaction, water. After 1 min, the reaction was stopped with EDTA. A 60-µl aliquot of the reaction mixture was pipetted onto a nitrocellulose membrane over suction. The vesicles were rinsed with 1 ml of the buffer containing 100 mM Na^+ to remove excess ^{22}Na. The membrane was transferred into an Eppendorf tube and 1 ml of scintillation liquid was added. The amount of the ^{22}Na isotope in the vesicles was determined by using a liquid scintillation counter (Beta Rack, Wallac). Usually 3–4 parallel measurements were done and the scintillation was counted also 3 or 4 times for each sample. A reaction standard was made using 10 µl of the reaction mixture on the membrane without rinsing.

4. Results and Discussion

4.1 Studies of the transport specificity of Na^+-PPases and Na^+,H^+-PPases (studies I and III)

Our strategy to study the ion transport specificity and evolution of Na^+-PPases and Na^+,H^+-PPases was to use well established kinetic and ion transport measurements combined with phylogenetic analyses and site-directed mutagenesis. In study I, the ion pumping specificity of Na^+-PPases was investigated and specific mutations were introduced to the *C. limicola* Na^+-PPase (Cl-PPase). Mutations were designed based on the newly published structure of Tm-PPase showing a water molecule near the ion gate (Figure 6). To study if the Na^+ ion binding site is located in place of the water molecule and to study the function of the ion gate, we designed mutations to see if they affect Na^+ binding or ion transport. In study III, the evolution of the ion transport specificity of Na^+-PPases and Na^+,H^+-PPases was analyzed by characterizing new enzymes that were located between the two enzyme families in the mPPase phylogenetic tree.

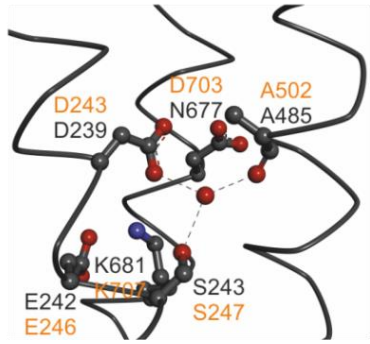

Figure 6. The structure of the Tm-PPase ion gate. Corresponding amino acid residues in Cl-PPase are marked in black. (Study I)

4.1.1 mPPase expression and isolation of IMVs (studies I and III)

Cl-PPase variant enzymes (Study I) and new wild-type mPPases, (Study III) were expressed in *E. coli* and isolated as inverted membrane vesicles (IMV). mPPases were visualized on Coomassie-stained SDS-PAGE gels. The calculated molecular mass of mPPase is approximately 75–80 kDa but due to the hydrophobicity of the proteins they migrate faster, at the rate of a 60–70-kDa protein. mPPases were also visualized by western blotting with an anti-H^+-PPase antibody. Furthermore, the effects of inhibitors on the hydrolysis activities of the new enzymes were measured. The mPPase inhibitor AMDP inhibited the hydrolysis, whereas the sPPase inhibitor KF had only a small inhibitory effect. This proved that the detected PP_i hydrolysis resulted from mPPase activity. Figure 7 shows the data for wild type and variant Cl-PPase enzymes. The variant enzymes K681R, D239S and D239E did not display any

detectable mPPase hydrolytic activity. The enzymes explored in Study III are displayed in Figure 8. Again, all new enzymes demonstrated a hydrolysis activity and were identified as functional mPPases.

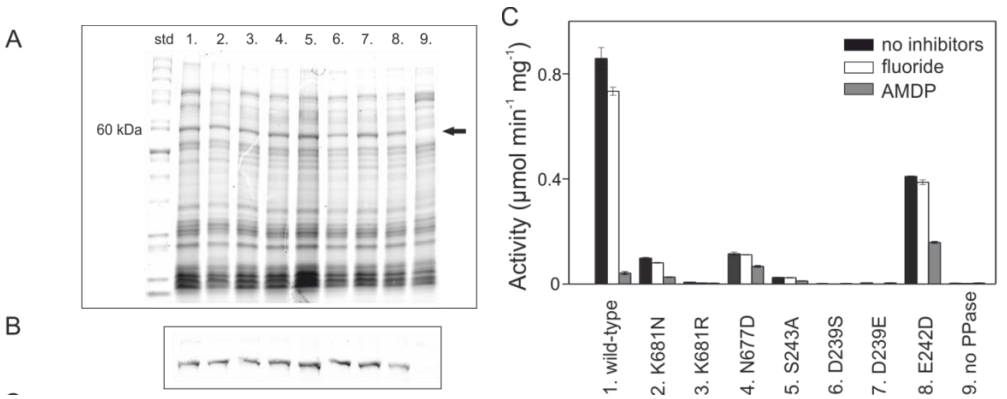

Figure 7. Four of the seven Cl-PPase variants had a PP_i hydrolysis activity**.** The expression of the wt and variant Cl-PPase enzymes was confirmed with a Coomassie stained SDS-PAGE gel (A) and by western blot (B). Hydrolysis activities were measured at 25 °C in the presence of the soluble PPase inhibitor KF and the mPPase inhibitor AMDP (C). The reaction mixture included 5 mM Mg^{2+}, 50 mM K^+, 10 mM Na^+, 100 µM Mg_2PP_i (pH 7.2). (Study I)

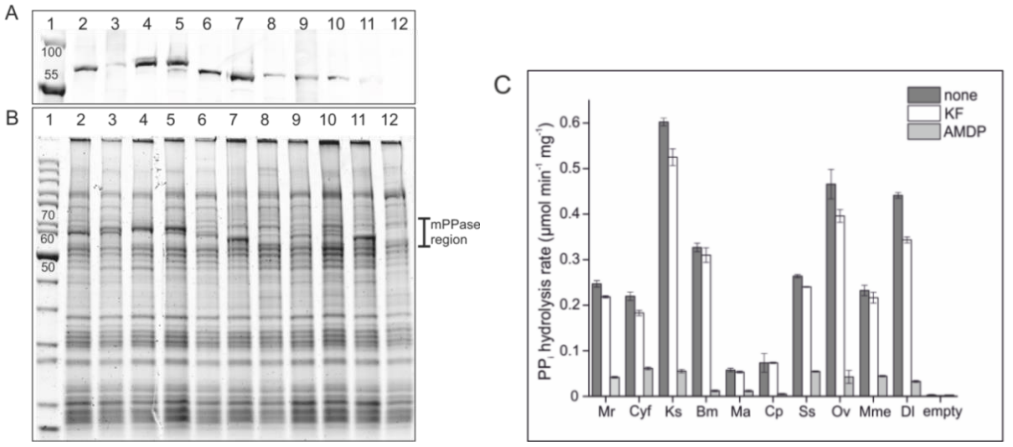

Figure 8. New enzymes were expressed as active mPPases. The expression of mPPases was verified with an anti-H^+-PPase antibody (A) and Coomassie-stained SDS-PAGE (B). PP_i hydrolysis activities were measured with inhibitors as indicated (C). (Study III)

4.1.2 Na^+-PPases can transport H^+ at low Na^+ concentrations (study I)

In study I, a major finding was that Na^+-PPases can transport H^+ ions at low Na^+ concentrations. The H^+-transport signal was seen when the Na^+ concentration was below 5 mM. The H^+ transport was measured for Cl-PPase at pH 6.2 and 8.2 in addition to pH 7.2 (Figure 9). At all tested pH values, the H^+ transport was seen when the Na^+ concentration was less than 5 mM and lowering the pH did not increase the H^+ pumping. Transport measurements with ionophores showed that the signal was electrogenic. CCCP abolished the signal, ETH157 did not affect it and valinomycin enhanced it (Figure 9 B). H^+ transport was measured also for other known Na^+-PPases and in all cases the H^+ transport was seen at 0.1 and 1 mM Na^+ concentrations but not for over 5 mM Na^+ concentrations (Figure 10). Thus, we concluded that H^+ transport at low Na^+ concentration is a common feature of all Na^+-PPases.

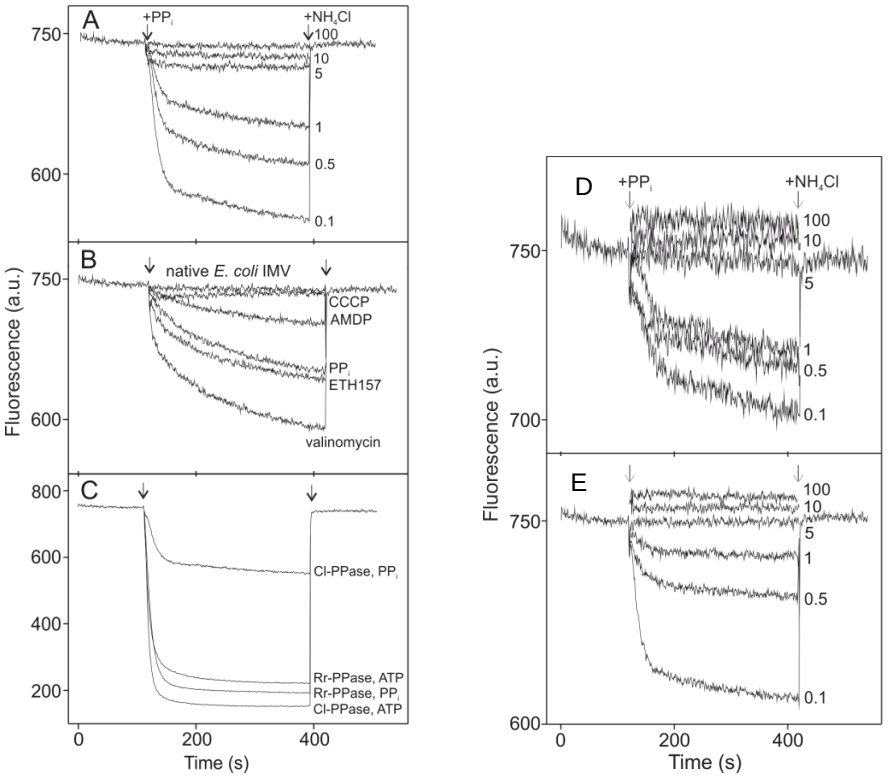

Figure 9. Na^+-PPases can transport H^+ ions at low Na^+ concentrations. A) The H^+ transport of Cl-PPase was measured at 5 mM Mg^{2+}, 50 mM K^+ and different Na^+ concentrations (indicated at the curves in mM). The additions of PP_i and NH_4Cl are indicated with arrows. B) The effects of ionophores and the mPPase inhibitor AMDP were measured at 0.1 mM Na^+. C) Rr-PPase was used for comparison. The H^+-transport of Cl-PPase was measured at pH 6.2 (D) and 8.2 (E). (Study I)

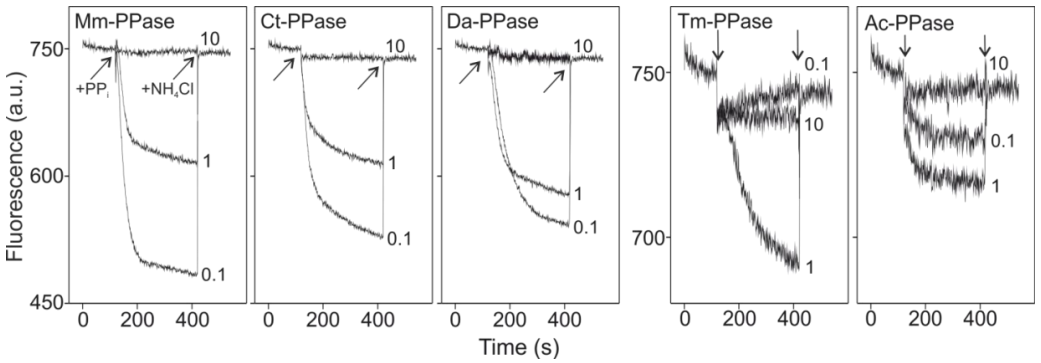

Figure 10. H^+ transport is a common feature of Na^+-PPases. The H^+ transport of different Na^+-PPases was measured at 0.1, 1 and 10 mM Na^+. (Study I)

4.1.2.1 Lys681 has an important role in H^+ transport in Cl-PPase

In study I, the Na^+ and H^+ ion transport of Cl-PPase variant enzymes was assayed. The K681R, D239E and D239S variants did not transport H^+ ions as expected since they did not have a PP_i hydrolysis activity. Other variants (E242D, S243A and N677D) transported H^+ ions, except for the K681N variant (Figure 11). The absence of H^+ pumping by the K681N variant was not due to a small hydrolysis activity because the K681N variant has an activity similar to that of the N677D variant, which showed H^+ pumping. Furthermore, the K681N variant transported Na^+ ions at the same rate as the other mutants. This indicates that the mutation affected only the H^+ transport but not the Na^+ transport function.

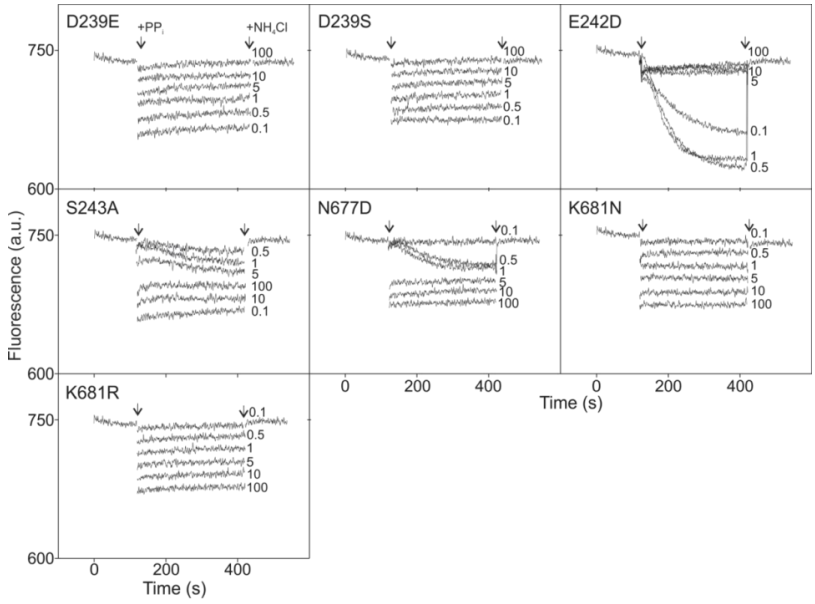

Figure 11. K681N variant enzyme is unable to transport H^+. H^+ transport was measured at different Na^+ concentrations for Cl-PPase variant enzymes.

Na^+ transport was measured with the ^{22}Na isotope. The accumulation of transported Na^+ into vesicles over time was measured for Cl-PPase in Study I (Figure 12A). The transport coupling ratio was calculated by dividing the amount of transported Na^+ by the amount of PP_i hydrolyzed in the same conditions (Figure 12B). The ratio (0.02 to 0.035) was constant over the range of Na^+ concentrations but very low, probably because of the leakiness of the *E. coli* membranes. The Na^+ transport of Cl-PPase variant enzymes was measured at different time points (Figure 13). The variants (K681R, D239S and D239E) that did not show any hydrolysis activity did not transport Na^+ ions either. The other variants (E242D, S243A, N677D and K681N) transported Na^+ ions increasingly over time. Importantly, the K681N variant was able to transport Na^+ ions, so the mutation affected only the H^+ transport activity.

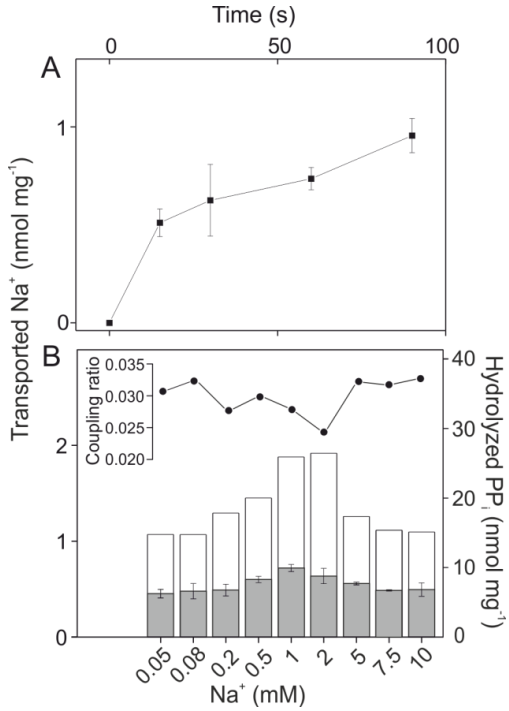

Figure 12. Na^+ accumulation by Cl-PPase was measured at different time points at 1 mM Na^+ (A) or at different Na^+ concentrations for a constant time (1 min) (B). The white bars represent the PP_i hydrolysis activity and the gray bars the amount of transported Na^+. (Study I)

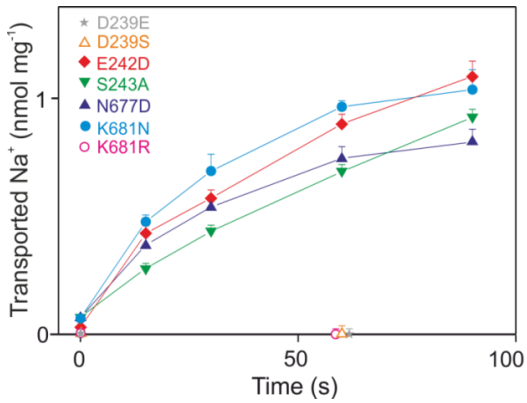

Figure 13. All Cl-PPases variants transport Na^+. The Na^+ transport by Cl-PPase variants was measured with 1 mM Na^+ over time. (Study I)

4.1.2.2 Activating Na^+ ion binds near the ion gate

In study I, Na^+ binding was measured for wild-type and variant Cl-PPase enzymes in the absence and presence of 50 mM K^+ (Figure 14). The mutations lowered the maximal activity compared to the wild type. Variant enzymes also required more Na^+ for activation.

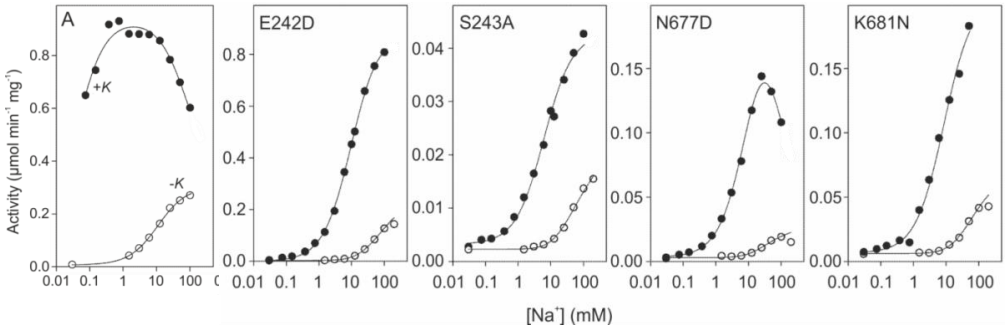

Figure 14. Mutations near the gate affect Na^+ binding. The hydrolysis activity was measured at different Na^+ concentrations for the wild-type Cl-PPase (A) and variant enzymes. Open circles represent activity measured in the absence of K^+ and closed circles in the presence of 50 mM K^+, respectively. (Study I)

All in all, our studies showed that the structure of the gate is very sensitive to changes in the amino acid residues. Furthermore, we showed that Lys681 has an important role in H^+ ion transport. Our mutational analysis revealed that Na^+-PPases have two Na^+-binding sites near the gate. The first Na^+-binding site activates PP_i hydrolysis and the second one controls ion transport. Furthermore, Na^+ and H^+ ions do not compete for the same transport machinery.

According to the proposed mechanism of ion translocation, Lys 681 has a key role in the different transport specificity of Na^+ -PPases and H^+-PPases (Li et al., 2016). Interestingly, Lys movement upon PP_i binding to Na^+-PPases makes space to bind the Na^+ ion to be transported (Figure 4B, D). However, when Na^+ is not bound to the gate, H^+ ion can be transported by Na^+-PPase. This explains why Na^+-PPases transport H^+ only at low Na^+ concentrations. The H^+ transport of Na^+-PPases is seen at sub-physiological Na^+ concentrations so that while it is mechanistically interesting, it probably has no physiological significance since the Na^+ concentration in the cell is rarely under 5 mM.

4.1.3 Na^+,H^+-PPases form two differently regulated groups (study III)

In study III, the H^+ transport of ten new enzymes from the Na^+-PPase and Na^+,H^+-PPase branches of the phylogenetic tree were characterized. The aim was to elucidate the ion pumping specificity and evolution of Na^+-PPases and Na^+,H^+-PPases. The H^+ pumping was assayed at different Na^+ concentrations from 0.1 mM to 100 mM (Figure 15). The new enzymes were divided into three groups based on their H^+ transport signal at different Na^+ concentrations. Enzymes that were not able to transport H^+ ions at Na^+ concentrations >5 mM were classified as Na^+-PPases, as defined in study I. Ks-, Bm-, Ss-, Ov-, Mme- and Dl-PPases were therefore identified as Na^+-PPases.

Enzymes that were able to transport H^+ ions at all tested Na^+ concentrations were classified as "true" Na^+,H^+-PPases (Mr- and Cyf-PPases). The H^+-transport of some enzymes was inhibited by Na^+ and they were classified as Na^+-regulated Na^+,H^+-PPases (Ma- and Cp-PPases). Also, the Na^+,H^+-PPases that were previously reported by Luoto et al. (2013), were studied more closely. As a result, Bv-, Am- and Po-PPases were classified as true Na^+,H^+-PPases and Clen- and Clep-PPases as Na^+-regulated Na^+,H^+-PPases.

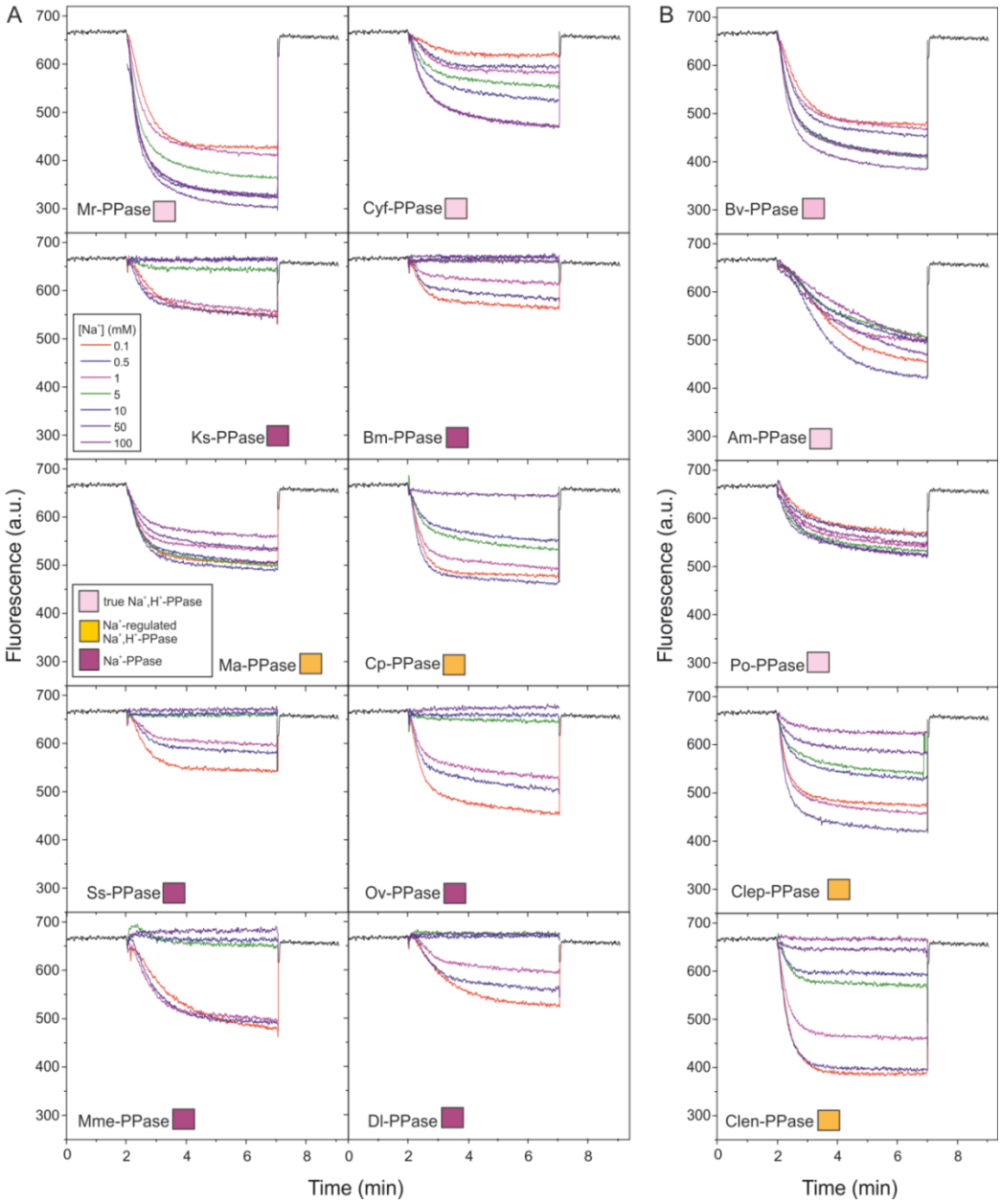

Figure 15. Na^+-PPases, Na^+ regulated Na^+,H^+-PPases and true Na^+,H^+-PPases are identified by their H^+ transport abilities. H^+-transport was measured at different Na^+ concentrations and the enzymes were divided into different subfamilies indicated with pink, yellow and purple for a true Na^+,H^+-PPase, a Na^+-regulated Na^+,H^+-PPase and a Na^+-PPase, respectively. (Study III)

In study III, all the new enzymes were shown to transport Na^+ (Figure 16). The Na^+-PPases and Na^+,H^+-PPases could not be separated based on the Na^+-transport data. Cl-PPase (a well-studied Na^+-PPase) was used as a positive control and an established H^+-PPase (Lb-PPase) as a negative control.

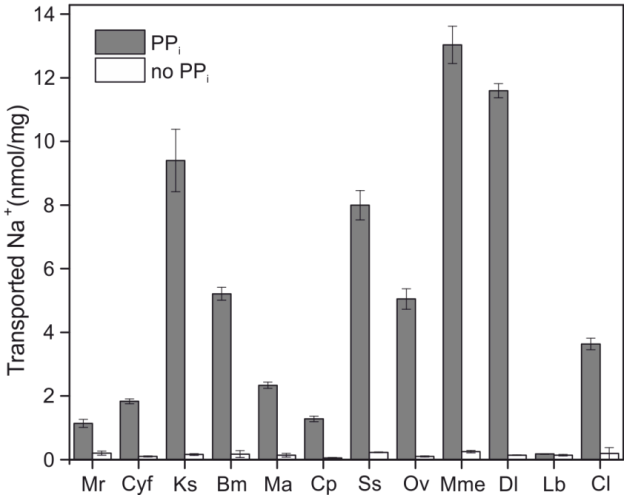

Figure 16. Na^+-PPases and Na^+,H^+-PPases cannot be separated based on Na^+ transport data. All new enzymes transported Na^+ ions. Lb-PPase was used as a negative control and Cl-PPase as a positive one. The error bars represent the SD of three independent measurements. (Study III)

The Na^+ dependence of PP_i hydrolysis was measured in the presence and absence of K^+ ions. In study III, all new enzymes were found to be Na^+ activated, as expected (Figure 17). K^+ further activated the enzymes and increased their affinity to Na^+. The Na^+ dependencies of Na^+-PPases and Na^+,H^+-PPases were similar. Both types of enzymes were activated by Na^+ and achieved their maximal activity in the presence of Na^+ and K^+. Our data on the effects of Na^+ and K^+ ions on the PP_i hydrolysis were in line with previous reports on Na^+-PPases and Na^+,H^+-PPases (Luoto et al., 2011, 2013; Malinen et al., 2007).

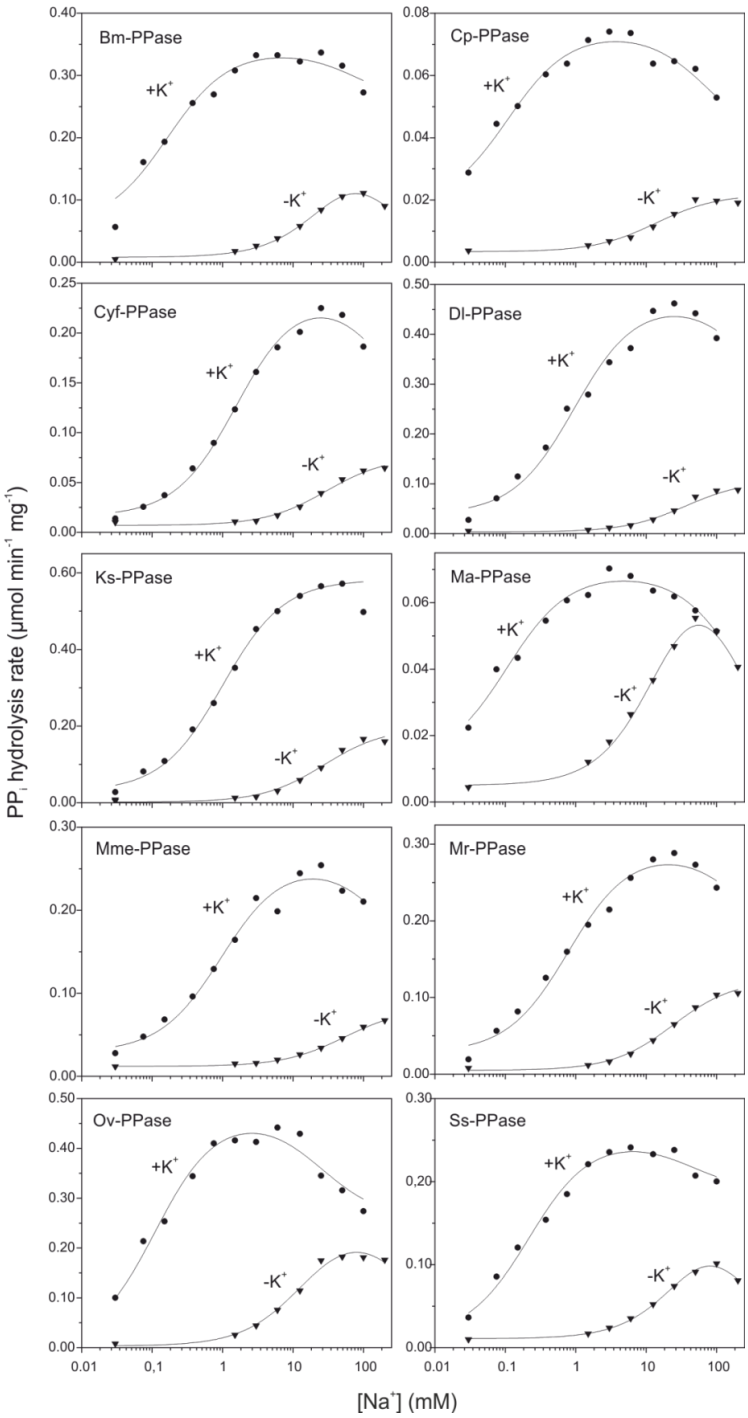

Figure 17. Na^+-dependence of PP_i hydrolysis was measured in the presence and absence of 50 mM K^+. (Study III)

4.2 Discovery of Na^+ regulated H^+-PPases (study II)

The aim of study II, was to determine if the enzymes in an evolutionarily divergent group are functional mPPases. A phylogenetic tree of all mPPases including the unidentified group of sequences was constructed (Figure 18). The tree showed a divergent group of sequences that was clearly distant from the other subfamilies. A sequence alignment revealed that the divergent mPPases possess the amino acid residues important for Mg_2PP_i binding. Interestingly, divergent mPPases have 100–150 extra amino acid residues compared to other prokaryotic mPPases. These extra residues are found in loops between TMHs and are predicted to form an extra TMH at the N-terminal end. Furthermore, divergent mPPases have Lys in the position were K^+-independent mPPases have Ala, which suggests that they are K^+-independent. Enzymes belonging to the divergent group from *C. limicola* and *Cellulomonas fimi* (Cl-PPase(2) and Cf-PPase, respectively) were chosen for characterization. The enzymes were cloned and expressed in *E. coli*. The enzymes showed a PP_i hydrolysis activity that was not inhibited by KF and AMDP. However, the antibody normally used to detect mPPases did not recognize the divergent mPPases, so they were visualized as His-tagged variants using an anti-His antibody (Figure 19).

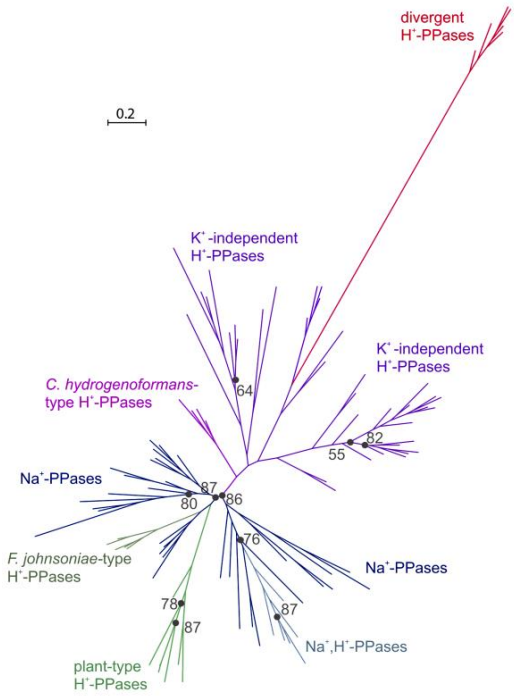

Figure 18. Phylogenetic tree of mPPases including a previously uncharacterized phylogenetically distant group of enzymes. (Study II)

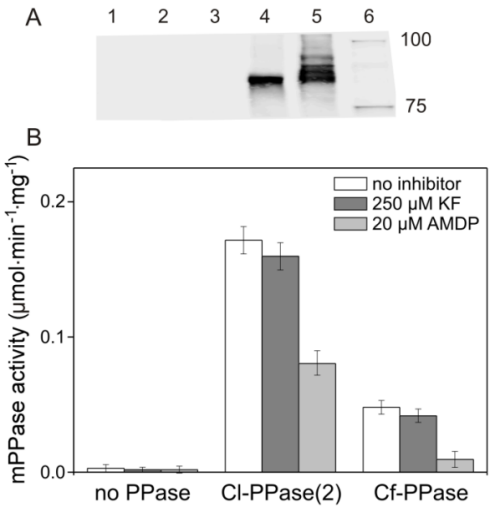

Figure 19. Divergent mPPases hydrolyze PPi. A) Western blot of divergent mPPases using an anti-His antibody. Order of the samples: 1. no-PPase 2. Cl-PPase(2) 3. Cf-PPase 4. His_8-tagged Cl-PPase(2) 5. His_8-tagged Cf-PPase 6. His_6 protein ladder B) The activities of Cl-PPase(2) and Cf-PPase were measured in the presence of 5 mM Mg^{2+}, 100 µM Mg_2PP_i and inhibitors. (Study II)

4.2.1 Divergent mPPases are H^+ transporters

Cl(2)-PPase and Cf-PPase both transport H^+ ions (Figure 20), but not Na^+ ions (Figure 21). The H^+ transport by Cl(2)-PPase was enhanced by K^+ and inhibited by Na^+. An H^+ transport signal was also seen with $DiBAC_4(3)$, which is an indicator of membrane potential. AMDP inhibited the H^+ transport by Cl-PPase(2). Na^+ transport was not seen with Cl-PPases(2), so we concluded that divergent mPPases are H^+ transporters.

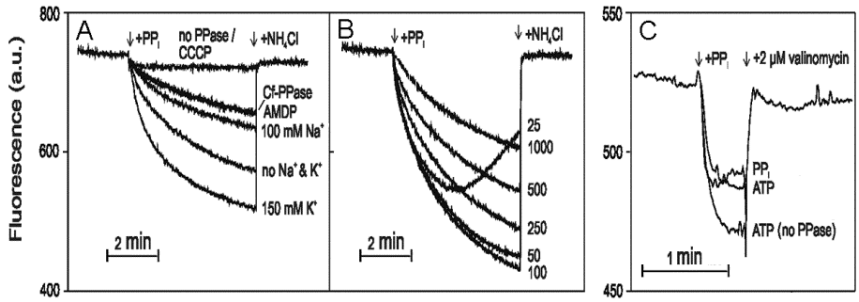

Figure 20. Divergent mPPases are H^+ transporters A) Cl-PPase(2) H^+-transport was measured with different added ions and ionophores as indicated at each curve B) Cl-PPase(2) H^+ transport at 25–1000 µM Mg2PPi. C) H^+ transport of Cl-PPase(2) measured with $DiBAC_4(3)$. (Study II)

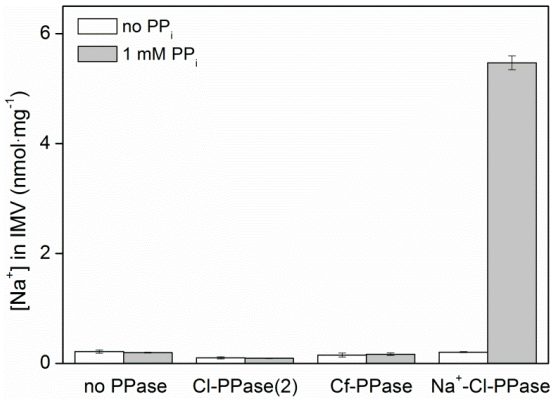

Figure 21. Cl-PPase(2) and Cf-PPase cannot transport Na^+ ions. The Na-PPase from *C. limicola* was used as a positive control. (Study II)

4.2.2 Discovery of a novel Na^+ regulation mechanism

Based on their sequence, divergent mPPases were expected to be K^+-independent. However, measurements showed that Cl-PPase(2) is activated by K^+ ions and inhibited by Na^+ ions. The effects of these ions depended on the substrate concentration (Figure 22). Furthermore, extensive kinetic measurements revealed that Na^+ and K^+ compete with Mg^{2+} ions for binding to the active site. Replacing the Mg^{2+} ion with K^+/Na^+ inhibited the enzyme especially at low substrate concentrations. However, at higher substrate concentrations K^+ activated the enzyme. The detailed kinetic characterization of Cl-PPase(2) can be found in the original publication of study II.

Interestingly, *C. limicola* has two different kinds of mPPases: a Na^+-PPase and a Na^+-regulated H^+-PPase. The Na^+ regulation of the H^+ transport may be used to regulate the activities of the two types of mPPases in the cell. The Na^+ inhibition mechanism of Cl-PPase(2) may thus ensure that at a high and toxic Na^+ concentration, the cell can use the available PP_i pool to pump Na^+ out of it, instead of consuming PP_i to transport H^+ ions.

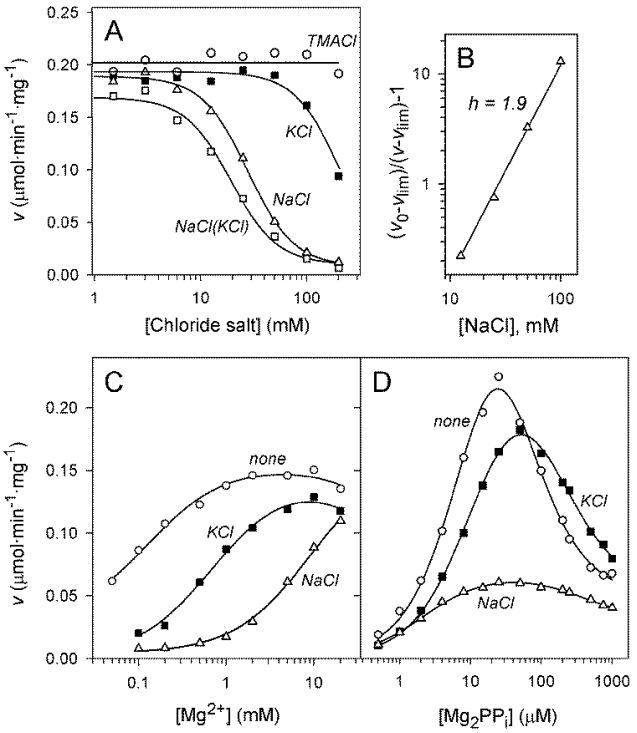

Figure 22. Cl-PPase(2) is regulated by K^+ and Na^+ ions. A) The effects of KCl and NaCl were measured with 20 µM Mg_2PP_i and 1 mM Mg^{2+}. The curve labelled as NaCl(KCl) shows the NaCl dependence measured in the presence of 50 mM KCl. TMACl was used to maintain a constant ionic strength. B) A hill plot of the NaCl data shown in panel (A). C) The effect of Mg^{2+} was measured with 20 mM Mg2PPi. 50 mM Na^+ and K^+ were added as indicated on the curves. D) The substrate dependence was measured with 5 mM Mg^{2+}. Na^+ (100 mM) and K^+ (150 mM) were added as indicated on the curve. (Study II)

4.3 Studies of the K^+ ion dependence of mPPase subfamilies (study IV)

In study IV, we explored the evolutionary conservation of K^+ dependence/ independence across the mPPase protein family. An attractive hypothesis for the major sequence determinant of the K^+ dependence/independence had been proposed previously based on the finding that an Ala460→Lys substitution in a K^+-dependent H^+-PPase from *C. hydrogenoformans* rendered the enzyme K^+-independent (Belogurov and Lahti, 2002). We wanted to expand the study of the K^+ dependence to mPPases from all subfamilies. We performed the Ala→Lys mutation in five enzymes that represented different K^+-dependent mPPase subfamilies. Furthermore, the reverse mutation Lys→Ala was introduced to a K^+-independent H^+-PPase and a Na^+-regulated H^+-PPase to test if they became K^+-dependent.

The chosen wild-type enzymes represented all of the different mPPase subfamilies. Dh-PPase and Gs-PPase were characterized for the first time in study IV. Other wild-type enzymes, Da-PPase (Luoto et al., 2011), Bv-PPase (Luoto et al., 2013), Fj-PPase (Luoto et al., 2011), Lb-PPase (Luoto et al., 2011) and Cl(2)-PPase (study II), had been previously characterized. Two new wild-type enzymes and five variants were all expressed in *E. coli* (Figure 23).

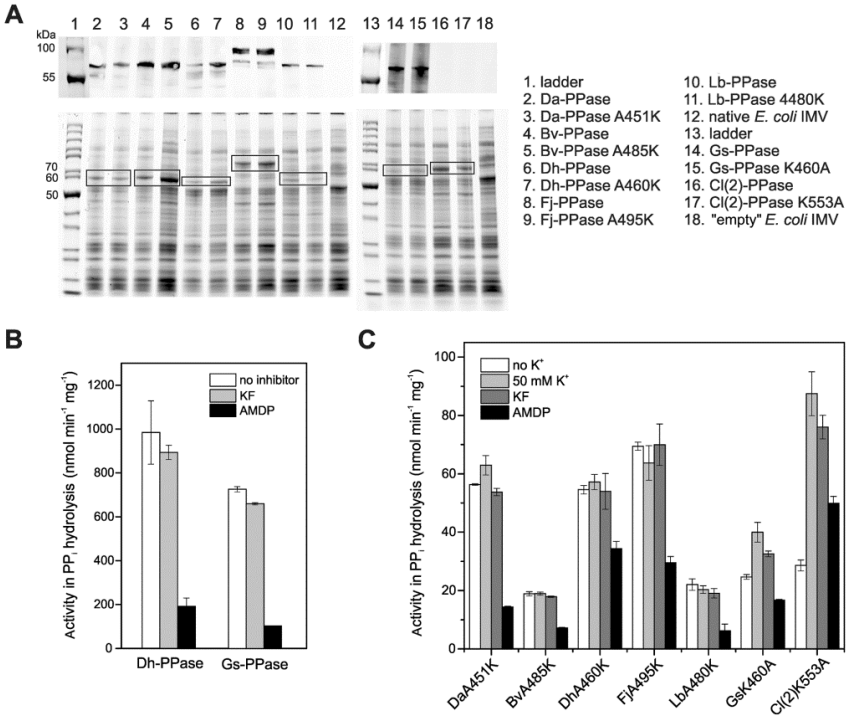

Figure 23. Wild-type and variant enzymes were detected with western blot and SDS-PAGE (A). Two new wild-type (B) and seven variant enzymes (C) actively hydrolyzed PP_i. (Study IV)

4.3.1 The K^+/Lys center determines K^+ dependence in all subfamilies

K^+-dependent H^+-PPases absolutely require millimolar concentrations of K^+ for their activity. Na^+-PPases achieve their maximal activity in the presence of K^+ and Na^+ but have some activity also with Na^+ only. To study the effects of the mutations, the K^+ activation of wild-type and variant enzymes was measured (Figure 24). Equation 1 was derived for Scheme 1 and used to make the fittings. The fitting parameters are listed in Table 3. In all cases, the mutations lowered the PP_i hydrolysis activities of the variant enzymes compared to the wild-type ones.

Wild-type K^+-dependent H^+-PPases (Dh-, Fj- and Lb-PPases) were activated but the Ala → Lys variants of these enzymes were not activated by K^+. Wild-type Na^+-PPase (Da-PPase) and Na^+,H^+-PPase (Bv-PPase) were active in the presence of 10 mM Na^+ but were further activated by K^+. The Ala→Lys variants of these Na^+-dependent

enzymes were not activated by K^+ ions. Gs-PPase is a K^+-independent H^+-PPase and the activity of its wild-type form was not increased by K^+ ions. However, the GsK460A variant was activated by K^+. Cl-PPase(2) is a Na^+-regulated H^+-PPase that is slightly activated by K^+ ions. The K553A variant enzyme had only low activity when no K^+ ions were added, but it was clearly activated by added K^+.

Our measurements also revealed that K^+-dependent H^+-PPases demonstrate activity even in the absence of K^+. PP_i hydrolysis was measured for Dh, Fj and Lb-PPase with no K^+ added. Furthermore, a small AMDP-sensitive H^+ transport signal was observed with Dh-PPase in the absence of K^+. This indicates that K^+-dependent H^+-PPases surprisingly retain function in the absence of K^+ ions.

$$\begin{array}{ccccc} & \overset{K_1}{} & & \overset{K_2}{} & \\ \mathrm{ES} & \leftrightarrow & \mathrm{ESM} & \leftrightarrow & \mathrm{ESM_2} \\ \downarrow V_0 & & \downarrow V_1 & & \downarrow V_2 \end{array}$$

Scheme 1. K^+ and Na^+ binding to the enzyme–substrate complex.

$$v = (V_1 + V_0K_1/[\mathrm{M}] + V_2[\mathrm{M}]/K_2)/(1 + K_1/[\mathrm{M}] + [\mathrm{M}]/K_2) \qquad \text{(Eq. 1)}$$

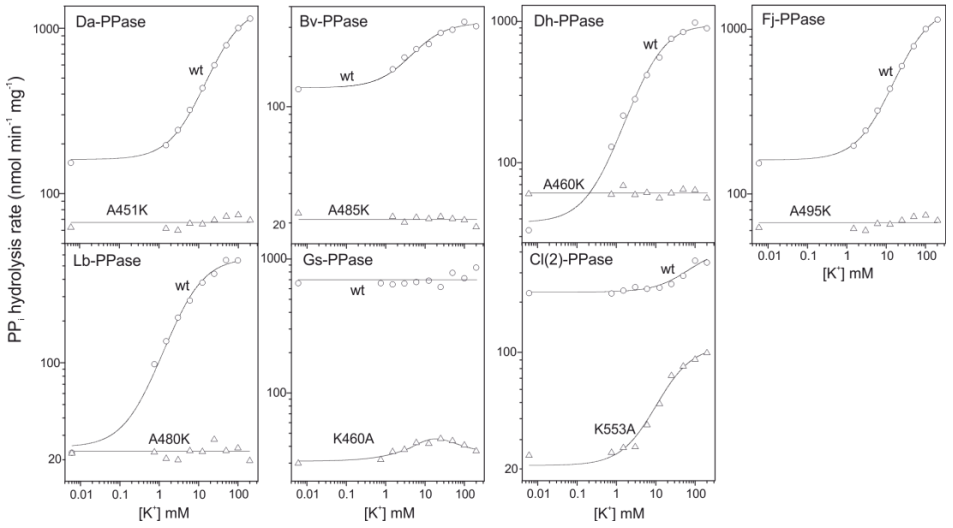

Figure 24. K^+ dependence of wild-type and variant mPPases. (Study IV)

Table 3. Kinetic parameters for the K^+ activation of PP_i hydrolysis at a fixed Mg_2PP_i concentration (100 μM). (Study IV)

Enzyme	V_0, nmol min^{-1} mg^{-1}	V_1, nmol min^{-1} mg^{-1}	V_2, nmol min^{-1} mg^{-1}	K_1, mM
Da[†]	160 ± 10	1360 ± 20	-	43 ± 2
Da (A451K)[*]	67 ± 2	-	-	-
Bv[†]	130 ± 10	320 ± 10	-	7 ± 2
Bv (A485K)[*]	21 ± 1	-	-	-
Dh	40 ± 10	970 ± 40	-	8 ± 1
Dh (A460K)	61 ± 1	-	-	-
Fj	20 ± 6	1170 ± 20	-	17 ± 1
Fj (A495K)	70 ± 3	<20	-	>100
Lb	25 ± 6	570 ± 20	-	6 ± 1
Lb (A480K)	23 ± 1	-	-	-
Gs	700 ± 20	-	-	-
Gs (K460A)	31 ± 2	70 ± 6	36 ± 3	16 ± 5[†]
Cl(2)	230 ± 10	420 ± 50	-	90 ± 50
Cl(2) (K553A)	21 ± 2	109 ± 4	-	23 ± 4

[*] The assay mixture additionally contained 50 mM Na^+.
[†] K_1 and K_2 values were arbitrarily assumed to be equal.

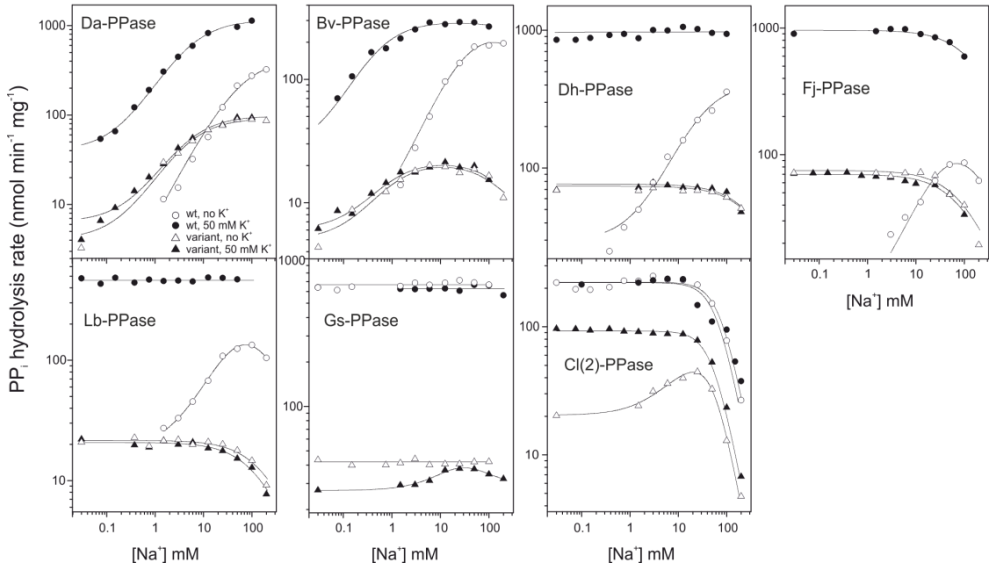

Figure 25. Na^+ dependence of wild-type and variant mPPases in the presence and absence of 50 mM K^+. (Study IV)

Na^+ activation was measured for all wild-type and variant enzymes in the presence and absence of 50 mM K^+ (Figure 25). In the absence of K^+, Na^+ was able to activate K^+-dependent enzymes. The Ala→Lys-mutated H^+-PPases (Dh-, Fj- and Lb-PPase) were not activated by Na^+ but instead inhibited by high Na^+ concentrations. In Na^+-

PPases and Na^+,H^+-PPases, K^+ enhanced Na^+ binding and increased the maximal catalysis rate. However, the Ala→Lys-mutated Na^+-dependent enzymes (Da- and Bv-PPases) were similarly activated in the presence and absence of K^+, indicating that the Lys replaced the activating function of the K^+ ion. The kinetic parameters describing these effects can be found in the original publication

4.3.2 Lys can functionally replace K^+ in ion transport

H^+ transport by the Ala→Lys-mutated enzymes was seen in the presence and absence of K^+ ions (Figure 26). The H^+ transport of the Lys→Ala variant enzymes was enhanced by K^+ ions. The Cl-PPase(2) K553A variant showed no H^+ transport in the absence of K^+ ions. The Gs-PPase K460A variant transported H^+ ions even in the absence of K^+ ions but the transport rate nearly doubled in the presence of K^+ ions. Dh-PPase also showed a small pumping signal in the absence of K^+ ions, which was abolished by AMDP. This further indicated that K^+ dependent H^+-PPases have a small activity even when no K^+ or Na^+ is available.

The Ala→Lys-mutated Da- and Bv-PPases were able to transport Na^+ in the absence of K^+ (Figure 27). As expected, the Ala→Lys variant of Lb-PPase was not able to transport Na^+, indicating that the K^+/Lys site does not control the ion pumping specificity.

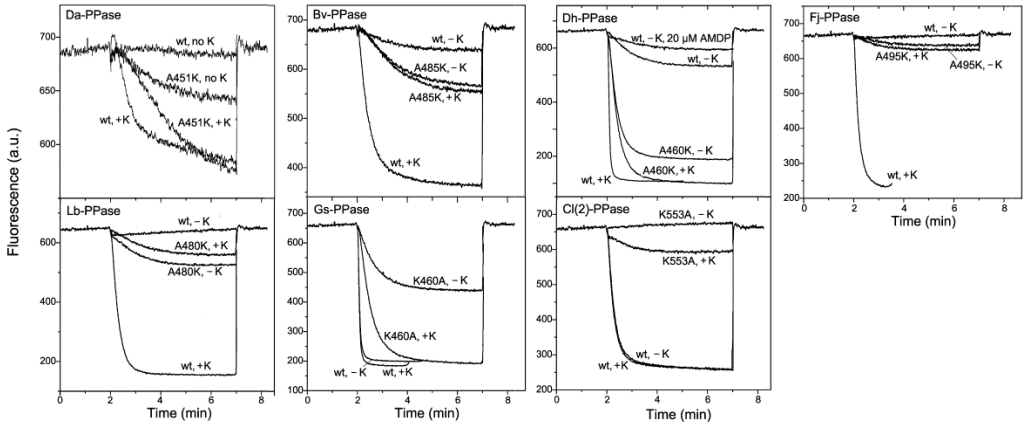

Figure 26. H^+ transport by wild type and variant enzymes was measured in the presence and absence of 50 mM K^+. (Study IV)

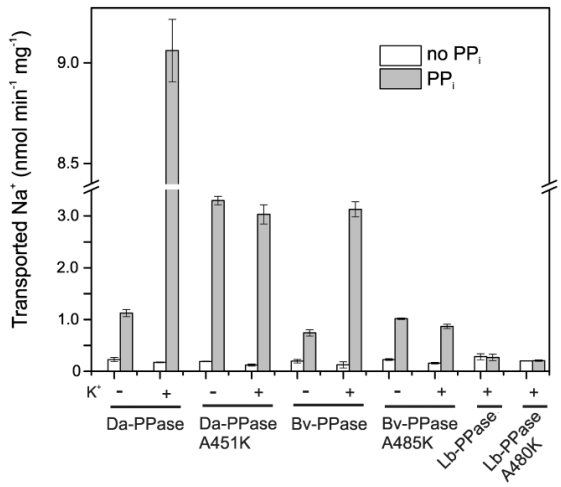

Figure 27. Na^+ transport by wild type and variant enzymes was measured in the presence and absence of 50 mM K^+. PP_i was replaced with water in the control reactions, white bars). (Study IV)

The effect of the K^+ ion on the conformation of the mPPases was tested using trypsin digestion. The PP_i hydrolysis activities of wild-type Dh-PPase and its A480K variant were measured in the absence and presence of 50 mM K^+ and 100 µM imidodiphosphate (IDP). The substrate analogue IDP protected the enzymes from digestion but the K^+ ion had no effect. Based on these results it seems that K^+ ion does not induce conformational changes in the structure of the mPPases.

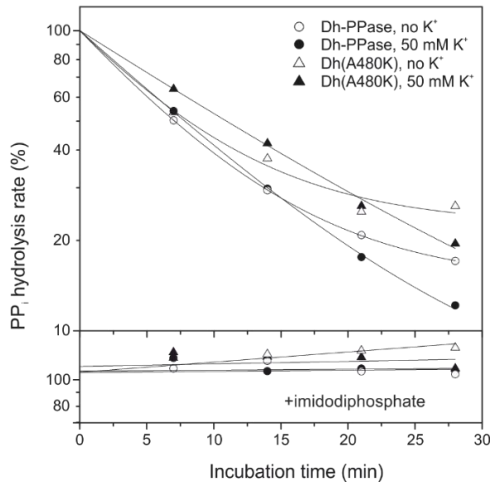

Figure 28. PP_i hydrolysis activity was measured at different time points during trypsin digestion (Study IV).

4.3.3 Substrate inhibition is a result of subunit asymmetry

The substrate (Mg_2PP_i) dependence of the hydrolysis of all wild type and variant enzymes was measured in the presence and absence of 50 mM K^+. Na^+ (10 mM) was added to Da- and Bv-PPases to keep these Na^+-transporting PPases active. Scheme 2 describes how the substrate binds to two subunits of the enzyme. Equation 2 was used to make the fittings in Figure 29. Surprisingly, a significant decrease in the activity of all wild type enzymes was observed at high substrate concentrations suggesting that the binding of the second substrate molecule partially arrests the enzyme. Because the mPPase active site has only space for one substrate molecule and there are no other potential PP_i binding sites, we concluded that the inhibition is due to substrate induced asymmetry in the function of the two subunits of the mPPase homodimer. At high substrate concentrations, substrate binding to one subunit interferes with substrate binding to the empty subunit. When both subunits are occupied by the substrate, the hydrolysis is slower. The inter-subunit regulation was only seen when the K^+/Lys site was working optimally. But when the site was mutated or empty (no K^+ bound) the substrate inhibition was not seen.

$$
\begin{array}{ccccc}
 & & K_{m1} & & \\
E_2 & & \leftrightarrow & E_2S & \rightarrow V_1 \\
K_{m1}\downarrow\uparrow & & K_{m2} & \downarrow\uparrow K_{m2} & \\
SE_2 & & \leftrightarrow & SE_2S & \rightarrow 2V_2 \\
\downarrow V_1 & & & &
\end{array}
$$

Scheme 2. Substrate binding and hydrolysis in two active sites of a dimeric mPPase.

$$v = (2V_1 + 2V_2[S]/K_{m2})/(2 + K_{m1}/[S] + [S]/K_{m2}) \qquad \text{(Eq. 2)}$$

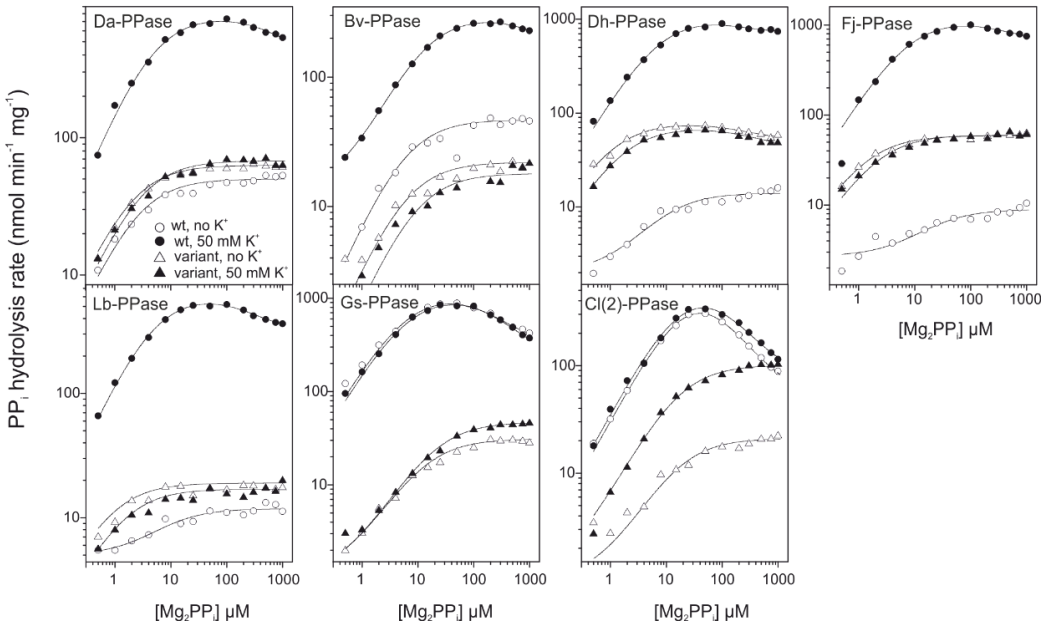

Figure 29. PP_i hydrolysis activity was measured at different substrate concentrations for wt and variant enzymes in the presence and absence of 50 mM K^+. For Da-PPase and Bv-PPase, 10 mM Na^+ was added to all reactions. (Study IV)

4.4 Phylogenetic tree of mPPases

A phylogenetic tree of all mPPases was constructed in study III (Figure 30 A). Table 4 summarizes all of the new mPPase wild type and variant enzymes characterized in studies I-IV. The results gained in this thesis elucidate the most complete picture of mPPase subfamilies and evolution so far.

Na^+-PPases are probably the evolutionary precursors of all mPPases (Luoto et al., 2011). In study I, we investigated the transport specificity of Na^+-PPases. We discovered that Na^+-PPases can transport protons at sub-physiological Na^+ concentrations. Furthermore, we identified a Lys residue that has an important role in the H^+ ion transport. We also identified two Na^+-binding sites that control the hydrolysis and ion transport, respectively. Our results support thus the theory that of H^+ transporting mPPases have evolved from Na^+ transporters.

In study II, the phylogenetic tree was expanded by identifying a new subfamily. We studied a phylogenetically divergent group of mPPases that was identified as Na^+-regulated H^+-PPases. This previously unknown group of enzymes has a unique mechanism of regulation.

In study III we investigated enzymes located between Na^+-PPases and Na^+,H^+-PPases on the phylogenetic tree. A detailed tree of the Na^+,H^+-PPase clade was also created, and based on their characteristics, the enzymes were divided into Na^+-PPases, true Na^+,H^+-PPases and Na^+-regulated Na^+,H^+-PPases (Figure 30 B). The tree shows that the Na^+,H^+ double-pumping ability has evolved twice in the nodes A and B and the two double-pumping subfamilies are separated by a group of Na^+-PPases. However, we were unable to identify distinct key amino acid residues that would explain the functional differences between the Na^+,H^+-PPases and Na^+-PPases. Furthermore, we concluded that the previously identified four signature residues (Luoto et al., 2013) are not limited to Na^+,H^+-PPases but are also found in some Na^+-PPases. This means that the significance of the signature residues was previously overestimated and the double-transport ability has probably evolved two times through several small amino acid residue changes that tuned the ion gate and the channel.

In study IV, the K^+ dependence was explored and was shown to be similarly conditioned in all subfamilies. All in all, our results indicate that Lys can functionally replace the K^+ ion in K^+-dependent H^+-PPases and Na^+-PPases. Furthermore, replacing the Lys with Ala confers K^+ activation to K^+-independent enzymes. We conclude that the K^+/Lys center is conserved across the different subfamilies and it has an important role in the communication between the subunits but has no effect on the ion transport specificity or mechanism.

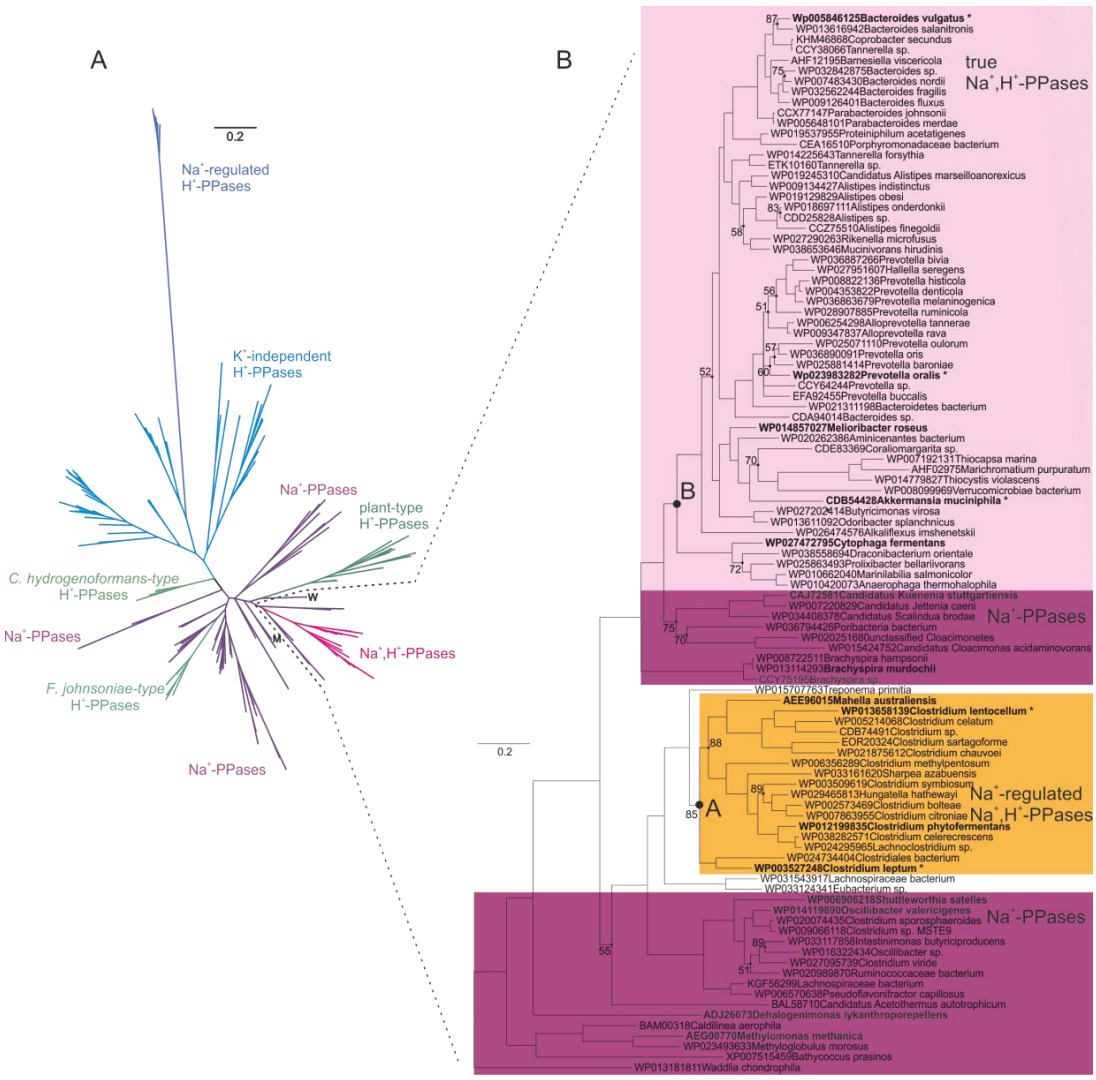

Figure 30. Phylogenetic tree showing all mPPase subfamilies (A) and a detailed tree of the Na^+,H^+-PPase branch (B). Clade credibility values below 90 are shown. The experimentally characterized mPPases are indicated in bold. (Study III)

Table 4. All new wild type and variant enzymes characterized in these studies.

Organism	**Abbreviation**	**Subfamily**	**NCBI number**	**Reference**
Chlorobium limicola	Cl(2)-PPase	Divergent H^+-PPase	WP012466119	Study II
Cellulomonas fimi	Cf-PPase	Divergent H^+-PPase	AEE45454	Study II
Brachyspira murdochii	Bm-PPase	Na^+,H^+-PPase	WP013114293	Study III
Candidatus Kuenenia stuttgartiensis	Ks-PPase	Na^+-PPase	CAJ72581	Study III
Cytophaga fermentans	Cyf-PPase	true Na^+,H^+-PPase	WP027472795	Study III
Clostridium phytofermentans	Cp-PPase	Na^+ regulated Na^+,H^+-PPase	WP012199835	Study III
Dehalogenimonas lykanthroporepellens	Dl-PPase	Na^+-PPase	ADJ26073	Study III
Mahella australiensis	Ma-PPase	Na^+ regulated Na^+,H^+-PPase	AEE96015	Study III
Melioribacter roseus	Mr-PPase	true Na^+,H^+-PPase	WP014857027	Study III
Methylomonas methanica	Mme-PPase	Na^+-PPase	AEG00770	Study III
Oscillibacter valericigenes	Oc-PPase	Na^+-PPase	WP014119890	Study III
Shuttleworthia satelles	Ss-PPase	Na^+-PPase	WP006906218	Study III
Geobacter sulfurredicencis	Gs-PPase	K^+ independent H^+-PPase	NP954331	Study IV
Desulfitobacterium hafniense	Dh-PPase	K^+ dependent H^+-PPase	BAE86625	Study IV
Variant enzymes	**Abbreviation**	**Mutation**	**Other**	**Reference**
C. limicola Na^+-PPase	Cl-PPase	S243A		Study I
		N677D		Study I
		K681N		Study I
		K681R	inactive	Study I
		D239S	inactive	Study I
		D239E	inactive	Study I
C. limicola H^+-PPase	Cl(2)-PPase	K553A		Study IV
G. sulfurredicencis	Gs-PPase	K460A		Study IV
Leptospira biflexa	Lb-PPase	A480K		Study IV
D. hafniense	Dh-PPase	A460K		Study IV
Bacteroides vulgatus	Bv-PPase	A485K		Study IV
Desulfuromonas acetoxidans	Da-PPase	A451K		Study IV
Flavobacterium johnsoniae	Fj-PPase	A495K		Study IV

5. Concluding remarks and future prospects

mPPases are a functionally versatile group of enzymes found in bacteria, archea, plants and protists. mPPases are potential drug targets against malaria and other protozoan diseases. Furthermore, mPPases offer possibilities for the biotechnical improvements of plants. Numerous studies have shown that overexpressing a vacuolar H^+-PPase is a productive approach for engineering stress-resistant plants. mPPases are interesting objects for the study of bioenergetics and evolution. mPPases have a unique structure but the mechanism of coupling PP_i hydrolysis to pumping and the ion transport specificity remain to be solved. A crystal structure of a Na^+,H^+-PPase would be helpful in elucidating the mechanism that determines the ion specificity.

In this research, the functional diversity of mPPases was studied by characterizing new enzymes, discovering new properties of known enzymes and defining completely new enzyme subfamilies. The results gained during this thesis project elucidate the functional properties of mPPases and also the evolutionary path of the ion pumping specificity of these primary transporters.

Acknowledgements

The research presented in this thesis was conducted in the Department of Biochemistry, University of Turku during the years 2013-2018. I would like to thank Professor Jyrki Heino for the excellent research environment. I thank the University of Turku Graduate School and Doctoral Programme of Molecular Life Science for funding my work as a PhD student.

Professors Masayoshi Maeshima and Aurelio Serrano are acknowledged for the pre-examination of this thesis. I thank Professor Markku Kulomaa for acting as the opponent.

I sincerely thank my supervisors Professor Reijo Lahti, Professor Alexander Baykov and Dr. Anssi Malinen for their guidance. I thank Dr. Anu Salminen and Dr. Saijaliisa Kangasjärvi for being members of my thesis advisory committee. I thank all the people who have worked in the POP laboratory during these years. Special thanks go to Heidi Luoto-Helminen. I would also like to acknowledge Anu Hirvensalo, Jani Sointusalo, Teija Luotohaara and Heli Kalevo for making the research work smooth by maintaining the research equipment and reagents.

I thank my fellow PhD students Tuuli, Matti, Kalle, Maria, Vilja, Pekka, Benjamin, Bikash, Natalia, Abbi, Johannes, Katri and Marjaana for their peer support and participation in our seminars. Special thanks go to Tuuli for the daily company at lunch, support and friendship. Last I would like to thank my family and most importantly my dear husband Kalle for his endless encouragement, support and love.

Turku, August 2018

Erika

References

Altschul, S.F., Gish, W., Miller, W., Myers, E.W., and Lipman, D.J. (1990). Basic Local Alignment Search Tool. J. Mol. Biol. *215*, 403–410.

Asaoka, M., Segami, S., and Maeshima, M. (2014). Identification of the critical residues for the function of vacuolar H^+-pyrophosphatase by mutational analysis based on the 3D structure. J. Biochem. *156*, 333–344.

Asaoka, M., Segami, S., Ferjani, A., and Maeshima, M. (2016). Contribution of PP_i-hydrolyzing function of vacuolar h^+-pyrophosphatase in vegetative growth of Arabidopsis: Evidenced by Expression of uncoupling mutated enzymes. Front. Plant Sci. *7*, 415.

Baltscheffsky, H., and Persson, B. (2014). On an early gene for membrane-integral inorganic pyrophosphatase in the genome of an apparently pre-LUCA extremophile, the archaeon *Candidatus Korarchaeum cryptofilum*. J. Mol. Evol. *78*, 140–147.

Baltscheffsky, H., Von Stedingk, L. V, Heldt, H.W., and Klingenberg, M. (1966). Inorganic pyrophosphate: formation in bacterial photophosphorylation. Science. *153*, 1120–1122.

Baykov, A.A., and Avaeva, S.M. (1981). A simple and sensitive apparatus for continuous monitoring of orthophosphate in the presence of acid-labile compounds. Anal Biochem *116*, 1–4.

Baykov, A.A., Bakuleva, N.P., and Rea, P.A. (1993a). Steady-state kinetics of substrate hydrolysis by vacuolar H^+-pyrophosphatase. Eur. J. Biochem. *217*, 755–762.

Baykov, A.A., Dubnova, E.B., Bakuleva, N.P., Evtushenko, O.A., Zhen, R.G., and Rea, P.A. (1993b). Differential sensitivity of membrane-associated pyrophosphatases to inhibition by diphosphonates and fluoride delineates two classes of enzyme. FEBS Lett. *327*, 199–202.

Baykov, A.A., Malinen, A.M., Luoto, H.H., and Lahti, R. (2013). Pyrophosphate-fueled Na^+ and H^+ transport in prokaryotes. Microbiol Mol Biol Rev *77*, 267–276.

Baykov, A.A., Anashkin, V.A., Salminen, A., and Lahti, R. (2017). Inorganic pyrophosphatases of Family II—two decades after their discovery. FEBS Lett. *591*, 3225–3234.

Belogurov, G.A., and Lahti, R. (2002). A lysine substitute for K^+. A460K mutation eliminates K^+ dependence in H^+-pyrophosphatase of *Carboxydothermus hydrogenoformans*. J Biol Chem *277*, 49651–49654.

Belogurov, G.A., Turkina, M. V., Penttinen, A., Huopalahti, S., Baykov, A.A., and Lahti, R. (2002). H^+-pyrophosphatase of *Rhodospirillum rubrum*. High yield expression in *Escherichia coli* and identification of the Cys residues responsible for inactivation by mersalyl. J. Biol. Chem. *277*, 22209–22214.

Belogurov, G.A., Malinen, A.M., Turkina, M. V, Jalonen, U., Rytkonen, K., Baykov, A.A., and Lahti, R. (2005). Membrane-bound pyrophosphatase of *Thermotoga maritima* requires sodium for activity. Biochemistry *44*, 2088–2096.

Biegel, E., and Muller, V. (2011). A Na^+-translocating pyrophosphatase in the acetogenic bacterium *Acetobacterium woodii*. J Biol Chem *286*, 6080–6084.

Bielen, A.A.M., Willquist, K., Engman, J., Van Der Oost, J., Van Niel, E.W.J., and Kengen, S.W.M. (2010). Pyrophosphate as a central energy carrier in the hydrogen-producing extremely thermophilic *Caldicellulosiruptor saccharolyticus*. FEMS Microbiol. Lett. *307*, 48–54.

Brini, F., Hanin, M., Mezghani, I., Berkowitz, G.A., and Masmoudi, K. (2007). Overexpression of

wheat Na^+/H^+ antiporter TNHX1 and H^+-pyrophosphatase TVP1 improve salt- and drought-stress tolerance in *Arabidopsis thaliana* plants. J. Exp. Bot. *58*, 301–308.

DeLano, W.L. (2002). PyMOL | pymol.org.

Docampo, R., and Moreno, S.N.J. (2011). Acidocalcisomes. Cell Calcium *50*, 113–119.

Drozdowicz, Y.M., and Rea, P.A. (2001). Vacuolar H^+ pyrophosphatases: from the evolutionary backwaters into the mainstream. Trends Plant Sci *6*, 206–11.

Drozdowicz, Y.M., Lu, Y.P., Patel, V., Fitz-Gibbon, S., Miller, J.H., and Rea, P.A. (1999). A thermostable vacuolar-type membrane pyrophosphatase from the archaeon *Pyrobaculum aerophilum*: implications for the origins of pyrophosphate-energized pumps. FEBS Lett *460*, 505–12.

Drozdowicz, Y.M., Kissinger, J.C., and Rea, P.A. (2000). H^+-translocating inorganic pyrophosphatase from *Arabidopsis*. Plant Physiol. *123*, 353–362.

Dudev, T., Musset, B., Morgan, D., Cherny, V. V., Smith, S.M.E., Mazmanian, K., Decoursey, T.E., and Lim, C. (2015). Selectivity mechanism of the voltage-gated proton channel, HV1. Sci. Rep. *5*, 1–11.

Edgar, R.C. (2004). MUSCLE: Multiple sequence alignment with high accuracy and high throughput. Nucleic Acids Res. *32*, 1792–1797.

Ferjani, A., Segami, S., Horiguchi, G., Muto, Y., Maeshima, M., and Tsukaya, H. (2011). Keep an eye on PP_i: the vacuolar-type H^+-pyrophosphatase regulates postgerminative development in Arabidopsis. Plant Cell *23*, 2895–2908.

Fukuda, A., Chiba, K., Maeda, M., Nakamura, A., Maeshima, M., and Tanaka, Y. (2004). Effect of salt and osmotic stresses on the expression of genes for the vacuolar H^+-pyrophosphatase, H^+-ATPase subunit A, and Na^+/H^+ antiporter from barley. J Exp Bot *55*, 585–594.

Gamboa, M.C., Baltierra, F., Leon, G., and Krauskopf, E. (2013). Drought and salt tolerance enhancement of transgenic *Arabidopsis* by overexpression of the vacuolar pyrophosphatase 1 (EVP1) gene from Eucalyptus globulus. Plant Physiol. Biochem. *73*, 99–105.

Gaxiola, R.A., Li, J., Undurraga, S., Dang, L.M., Allen, G.J., Alper, S.L., and Fink, G.R. (2001). Drought- and salt-tolerant plants result from overexpression of the AVP1 H^+-pump. Proc Natl Acad Sci U S A *98*, 11444–9.

Gaxiola, R.A., Regmi, K., and Hirschi, K.D. (2016). Moving On Up: H^+-PPase Mediated Crop Improvement. Trends Biotechnol. *34*, 347–349.

Gordon-Weeks, Koren'kov, Steele, and Leigh (1997). Tris is a competitive inhibitor of K^+ activation of the vacuolar H^+-pumping pyrophosphatase. Plant Physiol. *114*, 901–905.

Gordon-Weeks, R., Steele, S.H., and Leigh, R. a. (1996). The role of magnesium, pyrophosphate, and their complexes as substrates and activators of the vacuolar H^+-pumping inorganic pyrophosphatase (Studies Using Ligand Protection from Covalent Inhibitors). Plant Physiol. *111*, 195–202.

Hedlund, J., Cantoni, R., Baltscheffsky, M., Baltscheffsky, H., and Persson, B. (2006). Analysis of ancient sequence motifs in the H^+-PPase family. Febs J *273*, 5183–5193.

Heinonen, J.K. (2001). Biological Role of Inorganic Pyrophosphate (Boston, MA).

Hill, J.E., Scott, D. a, Luo, S., and Docampo, R. (2000). Cloning and functional expression of a gene encoding a vacuolar-type proton-translocating pyrophosphatase from *Trypanosoma cruzi*. Biochem. J. *351*, 281–288.

Hirono, M., and Maeshima, M. (2009). Functional enhancement by single-residue substitution of *Streptomyces coelicolor* A3(2) H^+-translocating pyrophosphatase. J. Biochem. *146*, 617–621.

Hirono, M., Ojika, M., Mimura, H., Nakanishi, Y., and Maeshima, M. (2003). Acylspermidine derivatives isolated from a soft coral, Sinularia sp, inhibit plant vacuolar H^+-pyrophosphatase. J Biochem *133*, 811–816.

Hirono, M., Mimura, H., Nakanishi, Y., and Maeshima, M. (2005). Expression of functional *Streptomyces coelicolor* H^+-pyrophosphatase and characterization of its molecular properties. J Biochem *138*, 183–191.

Hirono, M., Nakanishi, Y., and Maeshima, M. (2007a). Identification of amino acid residues participating in the energy coupling and proton transport of *Streptomyces coelicolor* A3(2) H^+-pyrophosphatase. Biochim. Biophys. Acta - Bioenerg. *1767*, 1401–1411.

Hirono, M., Nakanishi, Y., and Maeshima, M. (2007b). Essential amino acid residues in the central transmembrane domains and loops for energy coupling of *Streptomyces coelicolor* A3(2) H^+-pyrophosphatase. Biochim. Biophys. Acta - Bioenerg. *1767*, 930–939.

Holm, N.G., and Baltscheffsky, H. (2011). Links between hydrothermal environments, pyrophosphate, Na^+, and early evolution. Orig. Life Evol. Biosph. *41*, 483–493.

Huang, Y.-T., Liu, T.-H., Lin, S.-M., Chen, Y.-W., Pan, Y.-J., Lee, C.-H., Sun, Y.-J., Tseng, F.-G., and Pan, R.-L. (2013). Squeezing at entrance of proton transport pathway in proton-translocating pyrophosphatase upon substrate binding. J. Biol. Chem. *288*, 19312–19320.

Kajander, T., Kellosalo, J., and Goldman, A. (2013). Inorganic pyrophosphatases: One substrate, three mechanisms. FEBS Lett. *587*, 1863–1869.

Karlsson, J. (1975). Membrane-bound potassium and magnesium ion-stimulated inorganic pyrophosphatase from roots and cotyledons of sugar beet (*Beta vulgaris* L.). Biochim. Biophys. Acta *399*, 356–363.

Kellosalo, J., Kajander, T., Palmgren, M.G., Lopéz-Marqués, R.L., and Goldman, A. (2011). Heterologous expression and purification of membrane-bound pyrophosphatases. Protein Expr. Purif. *79*, 25–34.

Kellosalo, J., Kajander, T., Kogan, K., Pokharel, K., and Goldman, A. (2012). The structure and catalytic cycle of a sodium-pumping pyrophosphatase. Science (80-.). *337*, 473–476.

Khadilkar, A.S., Yadav, U.P., Salazar, C., Shulaev, V., Paez-Valencia, J., Pizzio, G.A., Gaxiola, R.A., and Ayre, B.G. (2016). Constitutive and companion cell-specific overexpression of *AVP1* , encoding a proton-pumping pyrophosphatase, enhances biomass accumulation, phloem loading, and long-distance transport. Plant Physiol. *170*, 401–414.

Kim, E.J., Zhen, R.G., and Rea, P.A. (1994). Heterologous expression of plant vacuolar pyrophosphatase in yeast demonstrates sufficiency of the substrate-binding subunit for proton transport. Proc Natl Acad Sci U S A *91*, 6128–32.

Kriegel, A., Andrés, Z., Medzihradszky, A., Krüger, F., Scholl, S., Delang, S., Patir-Nebioglu, M.G., Gute, G., Yang, H., Murphy, A.S., et al. (2015). Job sharing in the endomembrane system: vacuolar acidification requires the combined activity of V-ATPase and V-PPase. Plant Cell *27*, 3383–3396.

Laughlin, L.T., and Reed, G.H. (1997). The Monovalent cation requirement of rabbit muscle pyruvate kinase is eliminated by substitution of lysine for glutamate 117. Arch. Biochem. Biophys. *348*, 262–267.

Lee, C.H., Pan, Y.J., Huang, Y.T., Liu, T.H., Hsu, S.H., Lee, C.H., Chen, Y.W., Lin, S.M., Huang, L.K., and Pan, R.L. (2011). Identification of essential lysines involved in substrate binding of vacuolar H^+-pyrophosphatase. J. Biol. Chem. *286*, 11970–11976.

Leigh, R.A., Pope, A.J., Jennings, I.R., Sanders, D., Roles, T., Leigh, R.A., Pope, A.J., Jennings, I.R., and Sanders, D. (1992). Kinetics of the Vacuolar H^+-pyrophosphatase. *100*, 1698–1705.

Lemercier, G., Dutoya, S., Luo, S., Ruiz, F.A., Rodrigues, C.O., Baltz, T., Docampo, R., and Bakalara, N. (2002). A vacuolar-type H^+-pyrophosphatase governs maintenance of functional acidocalcisomes and growth of the insect and mammalian forms of *Trypanosoma brucei*. J Biol Chem *277*, 37369–37376.

Li, J., Yang, H., Peer, W.A., Richter, G., Blakeslee, J., Bandyopadhyay, A., Titapiwantakun, B., Undurraga, S., Khodakovskaya, M., Richards, E.L., et al. (2005). Arabidopsis H^+-PPase AVP1 regulates auxin-mediated organ development. Science (80-.). *310*, 121–125.

Li, K.-M., Wilkinson, C., Kellosalo, J., Tsai, J.-Y., Kajander, T., Jeuken, L.J.C., Sun, Y.-J., and Goldman, A. (2016). Membrane pyrophosphatases from *Thermotoga maritima* and *Vigna radiata* suggest a conserved coupling mechanism. Nat. Commun. *7*, 13596.

Lin, S.M., Tsai, J.Y., Hsiao, C.D., Huang, Y.T., Chiu, C.L., Liu, M.H., Tung, J.Y., Liu, T.H., Pan, R.L., and Sun, Y.J. (2012). Crystal structure of a membrane-embedded H^+-translocating pyrophosphatase. Nature *484*, 399–403.

Liu, J., Pace, D., Dou, Z., King, T.P., Guidot, D., Li, Z.-H., Carruthers, V.B., and Moreno, S.N.J. (2014). A Vacuolar-H^+-pyrophosphatase (TgVP1) is required for microneme secretion, host cell invasion, and extracellular survival of *Toxoplasma gondii*. Mol. Microbiol. *93*, 698.

Liu, L., Fan, X.D., Wang, F.W., Wang, N., Dong, Y.Y., Liu, X.M., Yang, J., Wang, Y.F., and Li, H.Y. (2013). Coexpression of ScNHX1 and ScVP in transgenic hybrids improves salt and saline-alkali tolerance in Alfalfa (*Medicago sativa* L.). J. Plant Growth Regul. *32*, 1–8.

López-Marqués, R.L., Pérez-Castiñeira, J.R., Losada, M., and Serrano, A. (2004). Differential regulation of soluble and membrane-bound inorganic pyrophosphatases in the photosynthetic bacterium *Rhodospirillum rubrum* provides insights into pyrophosphate-based stress bioenergetics. J. Bacteriol. *186*, 5418–5426.

Luecke, H. (1998). Proton transfer pathways in bacteriorhodopsin at 2.3 angstrom resolution. Science. *280*, 1934–1937.

Luoto, H.H., Belogurov, G.A., Baykov, A.A., Lahti, R., and Malinen, A.M. (2011). Na^+-translocating membrane pyrophosphatases are widespread in the microbial world and evolutionarily precede H^+-translocating pyrophosphatases. J Biol Chem *286*, 21633–21642.

Luoto, H.H., Baykov, A.A., Lahti, R., and Malinen, A.M. (2013). Membrane-integral pyrophosphatase subfamily capable of translocating both Na^+ and H^+. Proc Natl Acad Sci U S A *110*, 1255–1260.

Lv, S.L., Lian, L.J., Tao, P.L., Li, Z.X., Zhang, K.W., and Zhang, J.R. (2009). Overexpression of *Thellungiella halophila* H^+-PPase (TsVP) in cotton enhances drought stress resistance of plants. Planta *229*, 899–910.

Maeshima (1991). H^+-translocating inorganic pyrophosphatase of plant vacuoles. Eur. J. Biochem. *196*, 11–17.

Maeshima, M. (1990). Oligomeric structure of H^+-translocating inorganic pyrophosphatase of plant vacuoles. Biochem. Biophys. Res. Commun. *168*, 1157–1162.

Maeshima, M., and Yoshida, S. (1989). Purification and properties of vacuolar membrane proton translocating inorganic pyrophospatase from mung bean. J. Biol. Chem. *264*, 20068–20073.

Malinen, A.M., Belogurov, G.A., Baykov, A.A., and Lahti, R. (2007). Na^+-pyrophosphatase: a novel primary sodium pump. Biochemistry *46*, 8872–8878.

Malinen, A.M., Baykov, A.A., and Lahti, R. (2008). Mutual effects of cationic ligands and substrate on activity of the Na^+-transporting pyrophosphatase of *Methanosarcina mazei*. Biochemistry *47*, 13447–13454.

Mallo, N., Lamas, J., de Felipe, A.-P., Sueiro, R.-A., Fontenla, F., and Leiro, J.-M. (2016). Role of H^+-pyrophosphatase activity in the regulation of intracellular pH in a scuticociliate parasite of turbot: Physiological effects. Exp. Parasitol. *169*, 59–68.

Martin, M.B., Grimley, J.S., Lewis, J.C., Heath 3rd, H.T., Bailey, B.N., Kendrick, H., Yardley, V., Caldera, A., Lira, R., Urbina, J.A., et al. (2001). Bisphosphonates inhibit the growth of T*rypanosoma brucei*, *Trypanosoma cruzi*, *Leishmania donovani*, *Toxoplasma gondii*, and *Plasmodium falciparum*: a potential route to chemotherapy. J Med Chem *44*, 909–916.

Martinez, R., Wang, Y., Benaim, G., Benchimol, M., de Souza, W., Scott, D.A., and Docampo, R. (2002). A proton pumping pyrophosphatase in the Golgi apparatus and plasma membrane vesicles of *Trypanosoma cruzi*. Mol Biochem Parasitol *120*, 205–13.

McIntosh, M.T., Drozdowicz, Y.M., Laroiya, K., Rea, P.A., and Vaidya, A.B. (2001). Two classes of plant-like vacuolar-type H^+-pyrophosphatases in malaria parasites. Mol Biochem Parasitol *114*, 183–95.

Meng, X., Xu, Z., and Song, R. (2011). Molecular cloning and characterization of a vacuolar H^+-pyrophosphatase from *Dunaliella viridis*. Mol. Biol. Rep. *38*, 3375–3382.

Mimura, H., Nakanishi, Y., and Maeshima, M. (2005). Oligomerization of H^+-pyrophosphatase and its structural and functional consequences. Biochim Biophys Acta *1708*, 393–403.

Miroux, B., and Walker, J.E. (1996). Over-production of proteins in *Escherichia coli*: mutant hosts that allow synthesis of some membrane proteins and globular proteins at high levels. J Mol Biol *260*, 289–298.

Moyle, J., Mitchell, R., and Mitchell, P. (1972). Proton-translocating pyrophosphatase of *Rhodospirillum rubrum*. Febs Lett. *23*, 233–236.

Mulkidjanian, A.Y., Galperin, M.Y., Makarova, K.S., Wolf, Y.I., and Koonin, E. V (2008). Evolutionary primacy of sodium bioenergetics. Biol Direct *3*, 13.

Nakanishi, Y., Saijo, T., Wada, Y., and Maeshima, M. (2001). Mutagenic analysis of functional residues in putative substrate-binding site and acidic domains of vacuolar H^+-Pyrophosphatase. J. Biol. Chem. *276*, 7654–7660.

Nakanishi, Y., Yabe, I., and Maeshima, M. (2003). Patch clamp analysis of a H^+ pump heterologously expressed in giant yeast vacuoles. J Biochem *134*, 615–623.

Nelson, K.E., Clayton, R. a, Gill, S.R., Gwinn, M.L., Dodson, R.J., Haft, D.H., Hickey, E.K., Peterson, J.D., Nelson, W.C., Ketchum, K. a, et al. (1999). Evidence for lateral gene transfer between Archaea and bacteria from genome sequence of *Thermotoga maritima*. Nature *399*, 323–329.

Obermeyer, G., Sommer, A., and Bentrup, F.W. (1996). Potassium and voltage dependence of the inorganic pyrophosphatase of intact vacuoles from *Chenopodium rubrum*. Biochim. Biophys. Acta - Biomembr. *1284*, 203–212.

Oksanen, E., Ahonen, A.K., Tuominen, H., Tuominen, V., Lahti, R., Goldman, A., and Heikinheimo, P. (2007). A complete structural description of the catalytic cycle of yeast pyrophosphatase. Biochemistry *46*, 1228–1239.

Park, S., Li, J., Pittman, J.K., Berkowitz, G.A., Yang, H., Undurraga, S., Morris, J., Hirschi, K.D., and Gaxiola, R.A. (2005). Up-regulation of a H^+-pyrophosphatase (H^+-PPase) as a strategy to engineer drought-resistant crop plants. Proc Natl Acad Sci U S A *102*, 18830–18835.

Perez-Castineira, J.R., Lopez-Marques, R.L., Villalba, J.M., Losada, M., and Serrano, A. (2002). Functional complementation of yeast cytosolic pyrophosphatase by bacterial and plant H^+-translocating pyrophosphatases. Proc Natl Acad Sci U S A *99*, 15914–15919.

Pérez-Castiñeira, J.R., Hernández, A., Drake, R., and Serrano, A. (2011). A plant proton-pumping inorganic pyrophosphatase functionally complements the vacuolar ATPase transport activity and confers bafilomycin resistance in yeast. Biochem. J. *437*, 269–278.

Pizzio, G.A., Paez-Valencia, J., Khadilkar, A.S., Regmi, K., Patron-Soberano, A., Zhang, S., Sanchez-Lares, J., Furstenau, T., Li, J., Sanchez-Gomez, C., et al. (2015). Arabidopsis Type I proton-pumping pyrophosphatase expresses strongly in phloem, where it is required for pyrophosphate metabolism and photosynthate partitioning. Plant Physiol. *167*, 1541–1553.

Rauf, M., Saeed, N.A., Habib, I., Ahmed, M., Shahzad, K., Mansoor, S., and Ali, R. (2017). Isolation and in silico analysis of a novel H^+-pyrophosphatase gene orthologue from the halophytic grass Leptochloa fusca. J. Mol. Struct. *1129*, 179–187.

Rea, P.A., and Poole, R.J. (1986). Chromatographic resolution of h-translocating pyrophosphatase from H^+-translocating ATPase of higher plant tonoplast. Plant Physiol *81*, 126–129.

Rea, P.A., and Sanders, D. (1987). Tonoplast energization: Two H^+ pumps, one membrane. Physiol. Plant. *71*, 131–141.

Rea, P.A., Britten, C.J., Jennings, I.R., Calvert, C.M., Skiera, A., Leigh, R.A., Sanders, D., Rea, P.A., Britten, C.J., Jennings, I.R., et al. (1992). Regulation of vacuolar H^+-Pyrophosphatase by free calcium. Plant Physiol *100*, 1706–1715.

Regmi, K.C., Pizzio, G.A., and Gaxiola, R.A. (2016). Structural basis for the reversibility of proton pyrophosphatase. Plant Signal. Behav. *11*, e1231294.

Rodrigues, C.O., Scott, D.A., and Docampo, R. (1999). Characterization of a vacuolar pyrophosphatase in Trypanosoma brucei and its localization to acidocalcisomes. Mol. Cell. Biol. *19*, 7712–7723.

Ronquist, F., and Huelsenbeck, J.P. (2003). MrBayes 3: Bayesian phylogenetic inference under mixed models. Bioinformatics *19*, 1572–1574.

Ros, R., Romieu, C., Gibrat, R., And Grignon, C. (1995). The plant inorganic pyrophosphatase does not transport K^+ on vacuole membrane vesicles multilabled with fluorescent probes for H^+, K^+ and membrane potential. J. Biol. Chem. *270*, 4368–4374.

Sarafian, V., Kim, Y., Poole, R.J., and Rea, P.A. (1992). Molecular cloning and sequence of cDNA encoding the pyrophosphate-energized vacuolar membrane proton pump of *Arabidopsis thaliana*. Proc Natl Acad Sci U S A *89*, 1775–9.

Sato, M.H., Maeshima, M., Ohsumi, Y., and Yoshida, M. (1991). Dimeric structure of H^+-translocating pyrophosphatase from pumpkin vacuolar membranes. FEBS Lett. *290*, 177–180.

Sato, M.H., Kasahara, M., Ishii, N., Homareda, H., Matsui, H., and Yoshida, M. (1994). Purified

vacuolar inorganic pyrophosphatase consisting of a 75-kDa polypeptide can pump H^+ into reconstituted proteoliposomes. J. Biol. Chem. *269*, 6725–6728.

Schilling, R.K., Marschner, P., Shavrukov, Y., Berger, B., Tester, M., Roy, S.J., and Plett, D.C. (2014). Expression of the *Arabidopsis* vacuolar H^+-pyrophosphatase gene (AVP1) improves the shoot biomass of transgenic barley and increases grain yield in a saline field. Plant Biotechnol. J. *12*, 378–386.

Schilling, R.K., Tester, M., Marschner, P., Plett, D.C., and Roy, S.J. (2017). AVP1: One Protein, Many Roles. Trends Plant Sci. *22*, 154–162.

Schmidt, A.L., and Briskin, D.P. (1993). Energy transduction in tonoplast vesiclesd from red beet. Arch. Biochem. Biophys. *301*, 165–173.

Schöcke, L., and Schink, B. (1998). Membrane-bound proton-translocating pyrophosphatase of *Syntrophus gentianae*, a syntrophically benzoate-degrading fermenting bacterium. Eur. J. Biochem. *256*, 589–594.

Schultz, A., and Baltscheffsky, M. (2003). Properties of mutated *Rhodospirillum rubrum* H^+-pyrophosphatase expressed in *Escherichia coli*. Biochim. Biophys. Acta - Bioenerg. *1607*, 141–151.

Scott, D.A., de Souza, W., Benchimol, M., Zhong, L., Lu, H.G., Moreno, S.N., and Docampo, R. (1998). Presence of a plant-like proton-pumping pyrophosphatase in acidocalcisomes of *Trypanosoma cruzi*. J Biol Chem *273*, 22151–8.

Segami, S., Nakanishi, Y., Sato, M.H., and Maeshima, M. (2010). Quantification, organ-specific accumulation and intracellular localization of type II H^+-pyrophosphatase in *Arabidopsis thaliana*. Plant Cell Physiol. *51*, 1350–1360.

Segami, S., Tomoyama, T., Sakamoto, S., Gunji, S., Fukuda, M., Kinoshita, S., Mitsuda, N., Ferjani, A., and Maeshima, M. (2018). Vacuolar H^+-pyrophosphatase and cytosolic soluble pyrophosphatases cooperatively regulate pyrophosphate levels in *Arabidopsis thaliana*. Plant Cell *30*, 1040–1061.

Serrano, A., Perez-Castineira, J.R., Baltscheffsky, H., and Baltscheffsky, M. (2004). Proton-pumping inorganic pyrophosphatases in some archaea and other extremophilic prokaryotes. J Bioenerg Biomembr *36*, 127–133.

Seufferheld, M.J., Kim, K., Whitfield, J., Valerio, A., and Caetano-Anollés, G. (2011). Evolution of vacuolar proton pyrophosphatase domains and volutin granules: clues into the early evolutionary origin of the acidocalcisome. Biol. Direct *6*, 50.

Shah, N., Vidilaseris, K., Xhaard, H., and Goldman, A. (2016). Integral membrane pyrophosphatases: a novel drug target for human pathogens? AIMS Biophys. *3*, 171–194.

Shah, N.R., Wilkinson, C., Harborne, S.P.D., Turku, A., Li, K.M., Sun, Y.J., Harris, S., and Goldman, A. (2017). Insights into the mechanism of membrane pyrophosphatases by combining experiment and computer simulation. Struct. Dyn. *4*, 1–12.

Silva, P., and Gerós, H. (2009). Regulation by salt of vacuolar H^+-ATPase and H^+-pyrophosphatase activities and Na^+ /H^+ exchange. Plant Signal. Behav. *4*, 718–726.

Sosa, A., and Celis, H. (1995). H^+/PP_i stoichiometry of membrane-bound pyrophosphatase of *Rhodospirillum rubrum*. Arch. Biochem. Biophys. *316*, 421–427.

Sosa, A., Ordaz, H., Romero, I., and Celis, H. (1992). Mg^{2+} is an essential activator of hydrolytic activity of membrane-bound pyrophosphatase of *Rhodospirillum rubrum*. Biochem. J. *283*, 561–566.

Stamatakis, A., Hoover, P., and Rougemont, J. (2008). A rapid bootstrap algorithm for the RAxML

Web servers. Syst. Biol. *57*, 758–771.

Tsai, J.Y., Kellosalo, J., Sun, Y.J., and Goldman, A. (2014). Proton/sodium pumping pyrophosphatases: The last of the primary ion pumps. Curr. Opin. Struct. Biol. *27*, 38–47.

Tzeng, C.M., Yang, C.Y., Yang, S.J., Jiang, S.S., Kuo, S.Y., Hung, S.H., Ma, J.T., and Pan, R.L. (1996). Subunit structure of vacuolar proton-pyrophosphatase as determined by radiation inactivation. Biochem J *316*, 143–147.

Walker, R.R., and Leigh, R.A. (1981). Mg^{2+}-Dependent, cation-stimulated inorganic pyrophosphatase associated with vacuoles isolated from storage roots of red beet (*Beta vulgaris* L.). Planta *153*, 150–155.

White, P.J., Marshall, J., and Smith, J. a (1990). Substrate kinetics of the tonoplast H^+-translocating inorganic pyrophosphatase and its activation by free Mg^{2+}. Plant Physiol. *93*, 1063–1070.

Wu, J.J., Ma, J.T., and Pan, R.L. (1991). Functional size analysis of pyrophosphatase from *Rhodospirillum rubrum* determined by radiation inactivation. FEBS Lett. *283*, 57–60.

Yang, S.J., Jiang, S.S., Van, R.C., Hsiao, Y.Y., and Pan, R.L. (2000). A lysine residue involved in the inhibition of vacuolar H^+-pyrophosphatase by fluorescein 5'-isothiocyanate. Biochim. Biophys. Acta - Bioenerg. *1460*, 375–383.

Yang, S.J., Jiang, S.S., Hsiao, Y.Y., Van, R.C., Pan, Y.J., and Pan, R.L. (2004). Thermoinactivaion analysis of vacuolar H^+-pyrophosphatase. Biochim. Biophys. Acta - Bioenerg. *1656*, 88–95.

Yang, Y., Liu, Y., Yuan, H., Liu, X., Gao, Y., Gong, M., and Zou, Z. (2016). Membrane-bound pyrophosphatase of human gut microbe *Clostridium methylpentosum* confers improved salt tolerance in *Escherichia coli*, *Saccharomyces cerevisiae* and tobacco. Mol. Membr. Biol. *33*, 39–50.

Yoon, H.S., Kim, S.Y., and Kim, I.S. (2013). Stress response of plant H^+-PPase-expressing transgenic *Escherichia coli* and *Saccharomyces cerevisiae*: A potentially useful mechanism for the development of stress-tolerant organisms. J. Appl. Genet. *54*, 129–133.

Zhen, R.G., Baykov, a. a., Bakuleva, N.P., and Rea, P. a. (1994). Aminomethylenediphosphonate: A potent type-specific inhibitor of both plant and phototrophic bacterial H^+-pyrophosphatases. Plant Physiol. *104*, 153–159.

Annales Universitatis Turkuensis

Turun yliopisto
University of Turku

Painosalama Oy, Turku, Finland 2018

ISBN 978-951-29-7359-0 (PRINT)
ISBN 978-951-29-7360-6 (PDF)
ISSN 0082-7002 (PRINT) | ISSN 2343-3175 (PDF)